Frederico Cabral da Camara Oliveira Soares

Energy dissipation devices for structures under blast

Dissertação para obtenção do Grau de Mestre em
Engenharia Civil – Perfil Estruturas

Orientador: Professor Doutor Válter da Guia Lúcio,
Professor Associado, FCT/UNL

Co-orientador: Major Gabriel de Jesus Gomes, Exército Português

Juri:

Presidente: Prof. Doutor Corneliu Cismasiu

Arguente: Profª. Doutora Carla Alexandra da Cruz Marchão

Vogal: Prof. Doutor Válter José da Guia Lúcio

FACULDADE DE CIÊNCIAS E TECNOLOGIA
UNIVERSIDADE NOVA DE LISBOA

Janeiro 2018

Energy dissipation devices for structures under blast

ACKNOWLEDGMENTS

First and foremost, I would like to thank my scientific advisor Professor Válter Lúcio for the opportunity, trust, motivation and continuous support. I am very thankful for the knowledge I gained through this experience and for Prof. Válter Lúcio's availability throughout the entire process.

A special thanks to my scientific co-advisor, Engr. Major Gabriel Gomes for the assistance and knowledge provided.

I would also like to thank Prof. Rodrigo Gonçalves for all the help given with the computer program ADINA. Without this support it would not have been possible to complete this thesis.

Thank you to Captain José Pedro Basto, Captain João Marques, and to the Laboratory Technician José Gaspar for the support offered in Sta. Margarida's Military Camp. Thank you for making the tests possible. I would also like to acknowledge the company Concremat Lda for the manufacture of the test specimens, the company Orica Mining Services S.A. for providing the explosives, and the Portuguese Army, especially the Counter-IED and NBQR Centre of Excellence of the Engineering regiment nº 1 and to the Mechanised Brigade.

Thanks to Eng. Vitor Silva, for all the help in the laboratorial experiments done in the DEC.

To my rugby team, CDUL, thank you for understanding my absence from practice and social events during my thesis development.

Thanks to my parents, my brothers and sister for their support during my academic life.

Lastly, a special thanks to my girlfriend, Catarina, for all the support, patience and continuous encouragement in the last few years, particularly during my research and thesis process.

ABSTRACT

Terrorism pose a serious threat nowadays and many countries have the concern of protecting his people and most important buildings. This concern is an opportunity to strengthen the research of the behaviour of buildings under blast in order to reduce the magnitude of the effects of these catastrophic events.

The present thesis aims to create a functional system to improve the security of critical buildings, either new or adapting old buildings to receive this new system. This system also tries to be cost efficient, so this can be used in most buildings.

This thesis was centred in one system with two variations. The systems had the same lower reinforced concrete slab with 2,60 x 2,00 m and 0,12 m of thickness. The first system consisted in using 32 steel tubes of 76,1 mm outer diameter arranged uniformly and eight concrete panels, each one with 1,00 x 0,65 m and 0,07 m of thickness, on top of these tubes. The second system was the same concrete panels on top of 32 steel tubes with 48,3 mm outer diameter.

To test these systems four blast trials were prepared: the first is the reference specimen and the other two using the two mentioned variations of the system. These slabs were tested simply supported in two parallel edges, with a span of 2,30 m. In all tests 6,00 Kg of the explosive Eurodyn 2000 were used at a distance of 1,85 m from the top of the slab to the centre of the explosive. The results show an improvement in the residual deformation and on the opening of the visible cracks of the base reinforced concrete slab.

Keywords: Concrete plate, Energy dissipater, Steel tubes, Blast, Building blast protection

RESUMO

No mundo de hoje o terrorismo constitui uma séria ameaça e muitos países apresentam a preocupação de proteger as pessoas e os seus edifícios mais importantes. Esta preocupação é uma oportunidade para se reforçar o estudo da protecção dos edifícios contra explosões, de maneira a diminuir a magnitude dos efeitos destes eventos catastróficos.

A presente dissertação tem a intenção de criar um sistema funcional para melhorar a segurança dos edifícios estratégicos, sendo estes novos ou adaptados de edifícios antigos. Este sistema também tenta ser económico para que o sistema seja utilizado no maior número de edifícios.

Esta dissertação centrou-se num sistema com duas variações, ambas com a mesma laje inferior, em betão armado, com 2,60 x 2,00 m e 0,12 m de espessura. O primeiro sistema consistia em usar 32 tubos de aço com 76,1 mm de diâmetro exterior, dispostos uniformemente e oito placas, cada uma com 1,00 x 0,60 m e 0,07 m de espessura, posicionada sobre estes tubos. O segundo sistema tinha as mesmas oito placas sobre 32 tubos de aço com 48,3 mm de diâmetro exterior.

Para testar este sistema foram preparados quatro ensaios, sendo o primeiro com uma laje de referência e os outros dois usando as duas variações do sistema já mencionado. Estas lajes estavam simplesmente apoiadas em duas vigas paralelas, formando um vão de 2,30 m. Em todos os testes foram usados 6,00 Kg de explosivo Eurodyn 2000 a uma distância de 1,85 m entre o topo das lajes e o centro do explosivo. Os resultados mostraram um melhoramento na deformação residual e na abertura das fendas visíveis em relação à laje de referência.

Palavras-chave: Painel de betão, Dissipador de energia, Tubos de aço, Explosões, Proteção de edifícios contra explosões.

CONTENTS

LIST OF ILLUSTRATIONS

LIST OF TABLES

LIST OF ABBREVIATIONS AND ACRONYMS

Abbreviations

a	Deformation
A	Area
A_s	Area of steel in a reinforced concrete cross section
b	Width of a cross section
D	Tube diameter
d	Horizontal distance from both hinges
E_{cm}	Young modulus of concrete
E_p	Strain-hardening modulus
E_s	Young modulus of steel
f_{ck}	Characteristic value of the concrete stress resistance in compression for cylindrical specimens
f_{cm}	Average value of the concrete stress resistance in compression for cylindrical specimens
$f_{cm,cube}$	Average value of the concrete stress resistance in compression for cube specimens
$f_{cm,d}$	Average of the dynamic value of the concrete stress resistance in compression for cylindrical specimens
f_{ctm}	Average value of the concrete stress resistance in tension
$f_{ctm,d}$	Average of the dynamic value of the concrete stress resistance in tension
f_t	Maximum steel stress
f_y	Yielding steel stress
$f_{ym,d}$	Dynamic yielding steel stress
H	Hardness number of the material
h	Height
I_r	Reflected impulse
I_s	Specific shock wave impulse

L_w	Wave length
m	Mass
$M_{cr,d}$	Dynamic cracking moment
M_{eq}	Equivalent mass
M_p	Plastic moment
$M_{p,d}$	Dynamic plastic moment
M_y	Yielding moment
$M_{y,d}$	Dynamic yielding moment
P_0	Yielding load of the tube
P_a	Atmosphere pressure
P_r	Reflected overpressure peak value
P_p	Collapse load of the tube
P_{so}	Incident overpressure peak value
P_y	Yield force
R	Distance to the centre of the blast
ϱ	Density
σ_0	Yield stress
t	Wall thickness
T	Kinetic energy
t_0	Duration of the positive shock wave
U	Velocity of the wave
V_{eq}	Equivalent velocity
W	Absorbed energy
W_c	Bending modulus of the concrete cross section
W_{TNT}	Equivalent TNT weight of the explosive
Z	Scaled distance
θ	Rotation of the slab

Acronyms

BRDC	Blast resistant ductile connector
DIF	Dynamic increment factor
HSS	Hollow structural section
SIF	Strength increment factor
START	Study of Terrorism and Responses to Terrorism
TNT	Trinitrotoluene

1. INTRODUCTION

1.1. Blast threat

A statistic developed by Study of Terrorism and Responses to Terrorism (START) [1], presented in July 2017, shows that the terrorism is an everyday occurrence. According to this study in 2016 there were 11 072 terrorist attacks, that resulted in 25 621 deaths. The peak of deaths in the year of 2016 was in October of almost 100 deaths per day. To a rate of 2.4 deaths per attack the urge is massive to develop a system that can protect buildings and their users

The explosion of a bomb can induce enormous damages in his surroundings. Current buildings are not designed for the dynamic effects that an explosion introduces, what can destroy them. These dynamic effects are a shock wave, the expel of hot gases, ground vibrations and throw of materials, all of this in a split second. Most buildings are not prepared to face these, and these can result in a catastrophe.

1.2. Objectives

The objective of this thesis is to take an experimental campaign to study a system able to reduce the blast effects in buildings. This system is a precast concrete sandwich panel, composed by a "sacrificial layer" of steel tubes in between the two concrete plates. Two steel dimensions are studied: 48,3 mm of outer diameter and 2,6 mm of wall thickness and 76,1 mm of diameter and 3,2 mm of wall thickness.

The general objective, is to study how well this "layer" of tubes can dissipate the energy of an explosion, protecting the inner plate, or slab, from deforming and fail.

The research aims to study the efficiency of each tubes geometry used in large-scale models and how it can affect the mitigation of energy. It is also a major objective to test the viability of this system to be used as a protection against a terrorist attack.

1.3. **Organisation**

This thesis is divided in six chapters, including this one. In this first chapter it is done a presentation of the theme, and the objectives that the study wants to accomplish. The second chapter is composed by a bibliographic synthesis of the research work done along the years about the use of steel tubes and sacrificial layers to resist to dynamic or bomb forces. The third chapter the steel tubes used in the large-scale experiments are characterized by testing the steel in tension and in compression to understand how to quantify its energy dissipation capacity. In the fourth chapter the four large-scale models design, and production are presented, and the system used in the field tests is described. The fifth chapter presents the expected behaviour of the design slabs and tubes in the tests and of the real slabs and tubes, the analyses of the tests results, comparing the four tests results. In the sixth chapter the conclusions of the study are presented as well of some developments that can be done to improve the study on how the system can resist to a bomb attack. In the end there is two annexes to show the expected design of the large scale models and the tests explanation.

2. STATE OF ART

2.1. Introduction

Due to the devastating effects of an explosion and with the growing of terrorist threat, the possibility of mitigation the damage on buildings due to explosions has been studied by several authors. This chapter will describe the most relevant researches in the scope of this subject.

Therefore, an investigation of the inertia effects in one-dimensional metal ring systems. An analytical study on sacrificial claddings under blast loading will be presented. A large scale testing program of recyclable metal beverage cans. An experimental investigation about a mitigation of pressure impulses through blast resistant connectors. These studies improve the understanding in the capacity of energy dissipation and how can these tubular structures be used.

The characterization of the explosion is essential to ensure that the design of the system is the correct one. Some important characteristics are the peak pressure (P_{S0}) and the duration of the explosion, these parameters will be described in chapter 3.

2.2. Research Works

In 1983 Reid and Reddy [2] studied the inertia effect in a one-dimensional metal ring system subjected to end impact. The knowledge acquired with this experiment will allow us to predict and to see how this type of structures react to an impact situation.

The drop-hammer impact test was done on aluminium and mild-steel tubes, single and various layers. The details of the tubes are described on Table 2-1. In this table H is the hardness number of the material through a scale of

penetration of an indenter, the E_p is the strain-hardening modulus of the material, D is the diameter, t the thickness and b the extent of the ring.

Table 2-1 - Details of tube systems tested in [3]

Test	Material	System tested	Dimensions (mm)			Impact speed (ms^{-1})	Mass of hammer (kg)	Quasi-static material properties		
			D	t	b			H (kgf/mm^2)	σ_o (MPa)	E_p (GPa)
3	Mild-steel	Single tube	50	1,6	100	3,42	35,00	113	269	1,65
4	Mild-steel	Single tube	50	1,6	100	5,40	13,70	113	269	1,65
7	Aluminium	Single tube	50	1,6	100	2,18	35,00	34	100	1,24
8	Aluminium	Ten tubes in five layers	50	1,6	100	7,16	37,19	34	100	1,24

The conclusion of the impact speeds attainable using the drop hammer apparatus is that the response of a tube system can be deduced from that of a single tube by a scaling process equivalent to that demonstrated for quasi-static loading. The main reason for this was that, to a good approximation, the deformation is uniformly distributed throughout the system.

In Fig. 2-1 a) the response of the five-layered systems of aluminium tubes can be seen, and Fig. 2-1 b) shows the response of a single mild steel tube.

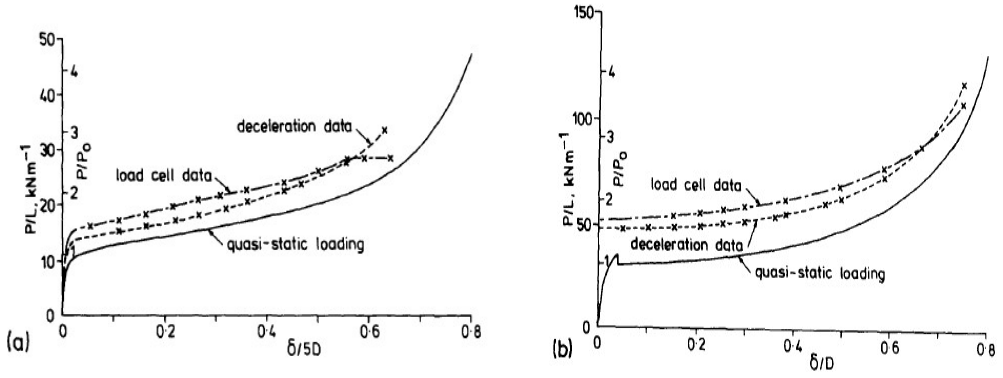

Fig. 2-1 - Force in load cell and hammer decelerating force vs system: a) Five-layer aluminium; b) single mild-steel tube [2]

In the vertical axis the P/L is the force divided by the length of the tubes, P/P_0 is the force divided by the initial collapse load. The horizontal axis is the total compression of the system divided by the diameter of the tubes multiplied by the number of layers.

The Fig. 2-2 shows a sequence of images of the deformation of the five-layer tubes. The mode of deformation of each tube is almost the same as seen during quasi-static compression. The deformation happens in an even way throughout the all system.

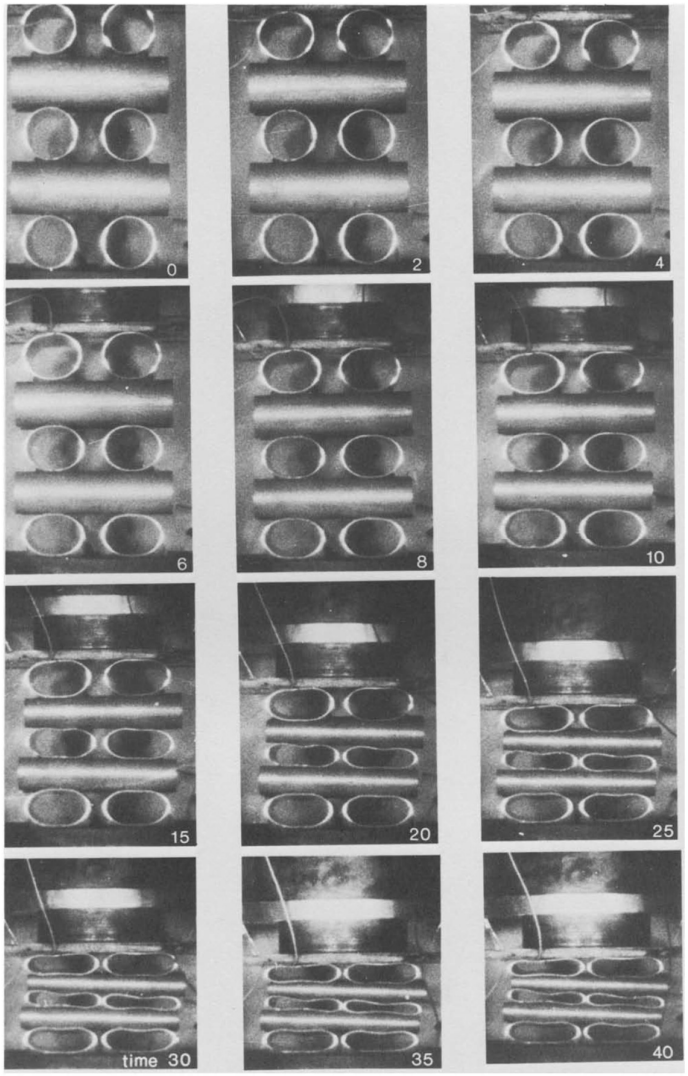

Fig. 2-2 - High speed film of deformation of five-layer aluminium tube [2]

To emphasise the effects of the inertia of tube-like systems, tests were done using the device shown in Fig. 2-3.

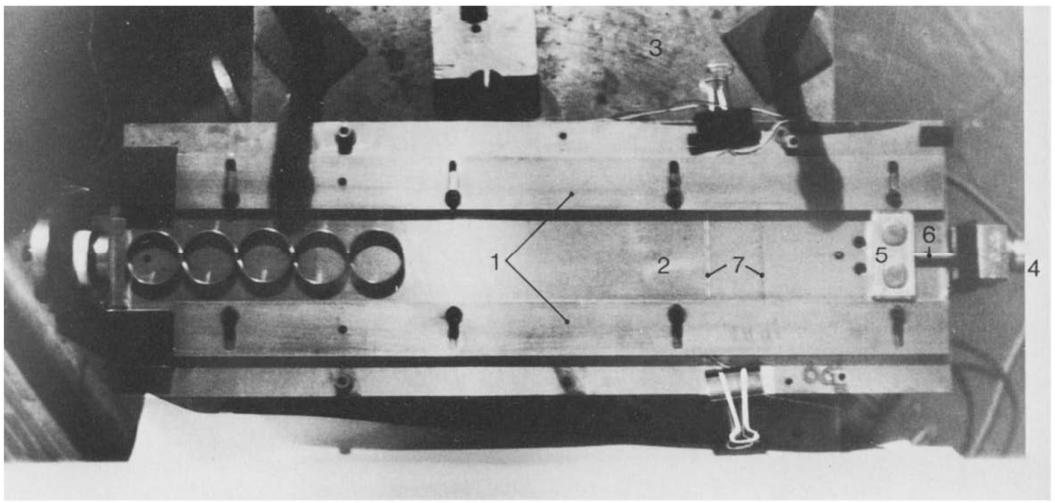

Fig. 2-3 - Sledge apparatus for high speed compression of ring systems [2]

The main quasi-static material properties can be deduced from the load-deflection curves for single rings laterally compressed between flat plates. These curves are presented in non-dimensional form in Fig. 2-3 and the main material and geometrical parameters are summarized in Table 2-1. These are derived from the following formula.

$$P_0 = \frac{\sigma_0 * t^2 * b}{\left(D - \frac{t}{2}\right)} \; [kN] \qquad \textbf{(2-1)}$$

Where P_0 is the collapse load of the ring, σ_0 is the yield stress of the material, D is the external radius, t the wall-thickness and b the extent of the ring.

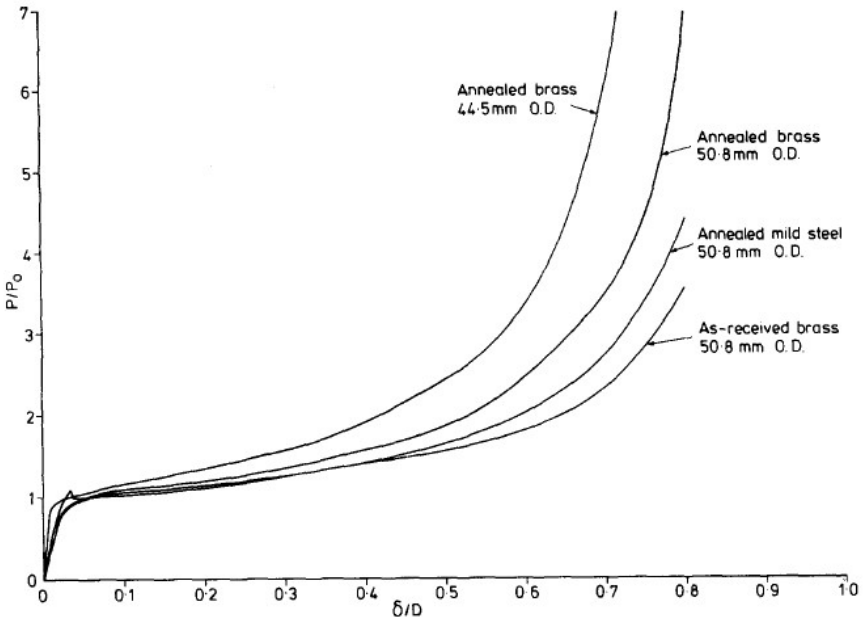

Fig. 2-4 - Non-dimensional quasi-static load-deflection curves for rings tested [2]

Numerous systems were tried to observe each response in function of impact speed, in the sledge mass and in the number of rings in the system as well as the material used.

Based on a quasi-static evaluation it would be expected that the response, of the tube-systems with numerous layers, of each ring would deform in the same extension and the deformation would decrease as the number of rings increased (Fig. 2-5). The first three systems show that expected behaviour, in a way that the first ring suffers less deformation as the number of rings increases from one to three. For the thicker rings there is a reduction on the level of deformation in the furthest ring, followed by an increase as the last one or two rings are reached.

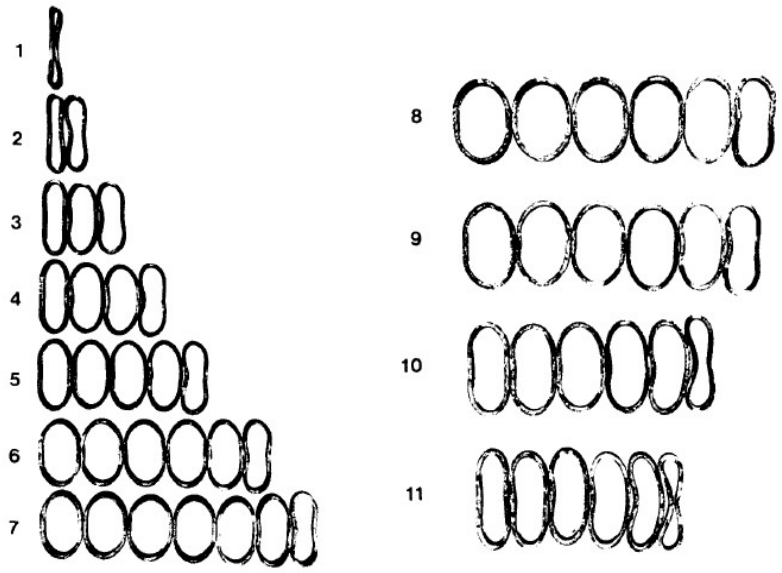

Fig. 2-5 - Deformed states of thick, annealed brass ring systems [2]

The inertia effect is higher when the impact tests speed was lower. The deformation of these systems, based in rings, is affected by the spread of a shock wave. The speed of the impact and the load ricochet of the ring are the controlling factors. The deformation is perhaps determined by the remaining kinetic energy in the system at the moment of the encounter of the reflected plastic wave and the shock wave. The systems with plates indicate how masses can be used to improve the distribution of deformation (Fig. 2-6).

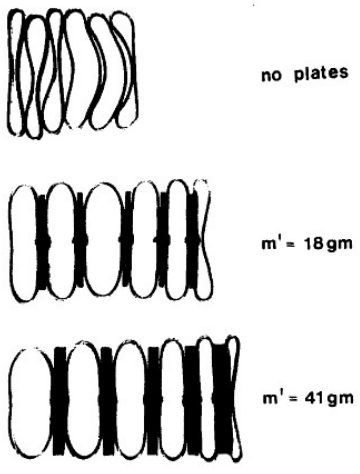

Fig. 2-6 - Deformation of the rings using plates and masses [2]

In 1999 Guruprasad and Mukherjee [4] [5] made a study showing the analytical model of a sacrificial cladding under a blast load. This paper shows how a structure behave while having a sacrificial cladding to a blast load.

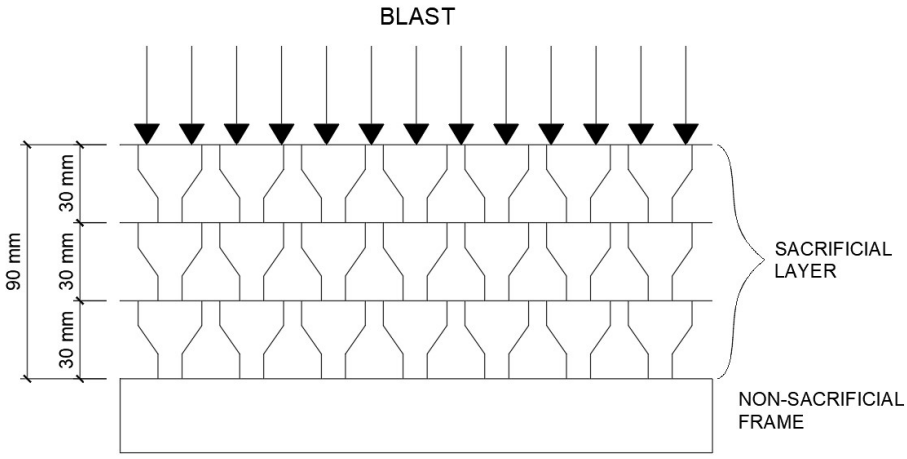

Fig. 2-7 - Layered design in Guruprasad and Mukherjee [4] [5]

The cladding layers are manufactured of thin mild steel sheets and the structure can be designed in two layers: a sacrificial and a non-sacrificial (Fig. 2-7).

The final configuration of this system (Fig. 2-7) needs to ensure three important aspects: there should be enough space available within each layer for large plastic deformations to take place; it is important that the layers should not break during the blast loading; and the layers should get crushed effectively and the pattern of deformation should remain unchanged every time for the expected blast loading. These three aspects are essential since it is the sacrificial cladding that dissipates the blast energy.

The analytical studies were carried out for single and three layer sacrificial claddings. The loads and structural details are presented in Table 2-2

Table 2-2 - Reflected overpressure [4] [5]

Case no.	Sheet thickness (mm)	No. of layers	Peak pressure (N/mm²)	Time duration (sec)
1	1,6	1	3,38	0,0010803
1a	1,6	3	3,38	0,0010803
2	1,6	1	5,35	0,0010815
2a	1,6	3	5,35	0,0010815
3	1,2 (1,6 web)	3	2,71	0,0014469
4	1,2	3	2,71	0,0014469

From Fig. 2-8 it can be concluded that a simple analytical model is able to predict the layer collapses accurately. The simple analytical model achieves a realistic distribution of mass by lumping the masses at very close intervals. This may be the key to the success of the simple model.

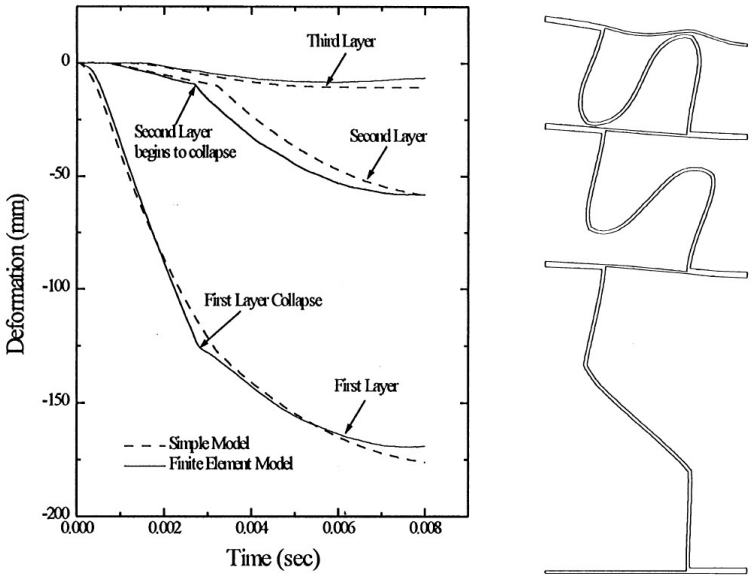

Fig. 2-8 - Deformation of three layers [4] [5]

The sacrificial layer configuration proposed in this paper is efficient. The simple analytical model and finite element model give similar results. The proposed layer configuration was found to be efficient in the dissipation of the blast. The layers of the sacrificial cladding collapse successively. The sacrificial layer effectively isolates the non-sacrificial structure from the blast.

In 2011, a group of engineers [6] tested a sacrificial cladding made of empty recyclable beverage cans in a large-scale air blast load. This study shows how an every-day object can be used for the protection of civil engineering structures.

They selected empty recyclable metal beverage cans. A special care was taken to choose cans without defects, so the tests won't be compromised. The cans chosen to the study were those from a combination of two materials, body in steel and the top cover made of aluminium (Fig. 2-9)

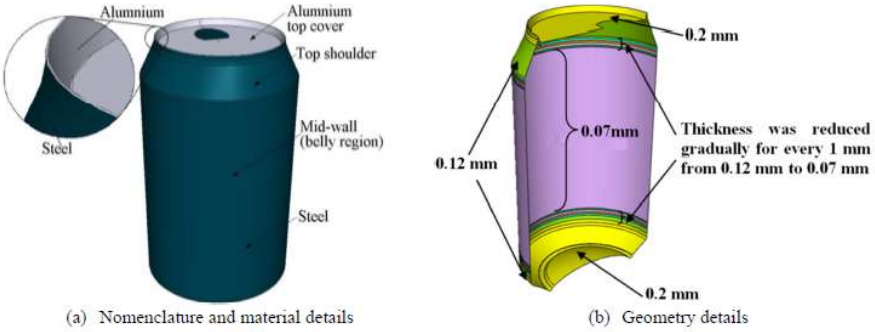

Fig. 2-9 - Material and geometry details of an empty metal beverage can [6]

They mounted the large-scale experiment as it can be seen in Fig. 2-10. Two plates were used, one in front and one in the back of the beverage cans. The font panel was instrumented with three pressure sensors and two accelerometers to measure the reflected pressure and the acceleration of the skin plate respectively. The back panel was instrumented with dynamic force sensors to measure the transferred impulse to the concrete structure. The C4 charge was located at the other end of the concrete pipe, 4,2 meters away. There were two configurations of the beverage cans (25 and 37 beverage cans) and three different weights of C4 charge (75g, 100g and 150g of C4).

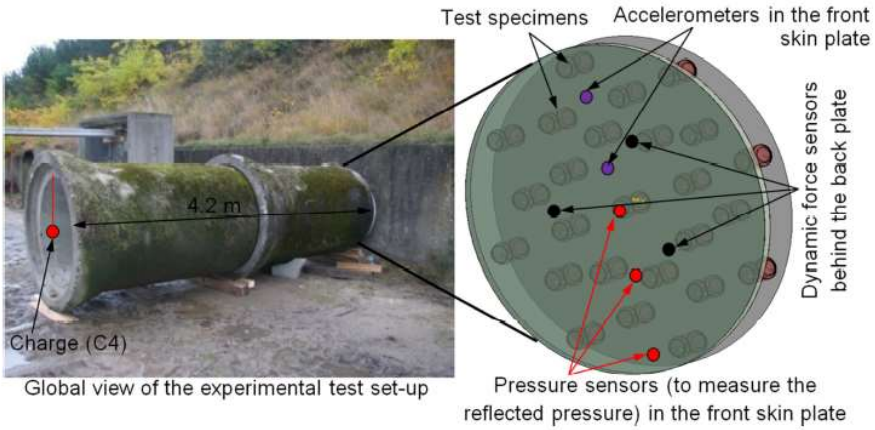

Fig. 2-10 - Global view of the large-scale experiment [6]

Fig. 2-11 shows the explosion of C4 and the propagation of the pressure wave inside the concrete pipes. In the same illustration can be seen a perfectly plane shock wave was formed at the other end of the tube.

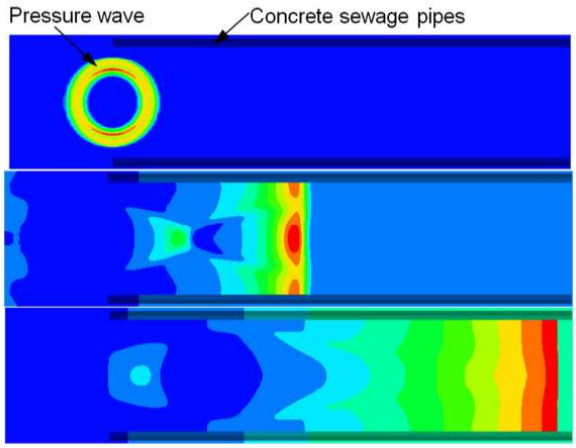

Fig. 2-11 - Propagation of blast pressure wave inside concrete sewage pipe [6]

All tests shown that the beverage cans crushed gradually during the blast load (Fig. 2-12). The beverage cans showed an asymmetric failure pattern, which depends on the combined effect of D/t ratio and the material strain hardening characteristics. The final deformation of the beverage cans is shown in Fig. 2-13 a). To compare the effectiveness of the proposed sacrificial cladding structure a reference test was conducted without the beverage cans (Fig. 2-13 b)) the charge and the distance for this test were the same as for the previous tests. The results

showed that the use of beverage cans reduces substantially the peak crush load and the duration of the event was extended considerably (Fig. 2-13 b)).

Fig. 2-12 - Progressive crushing stages of beverage cans [6]

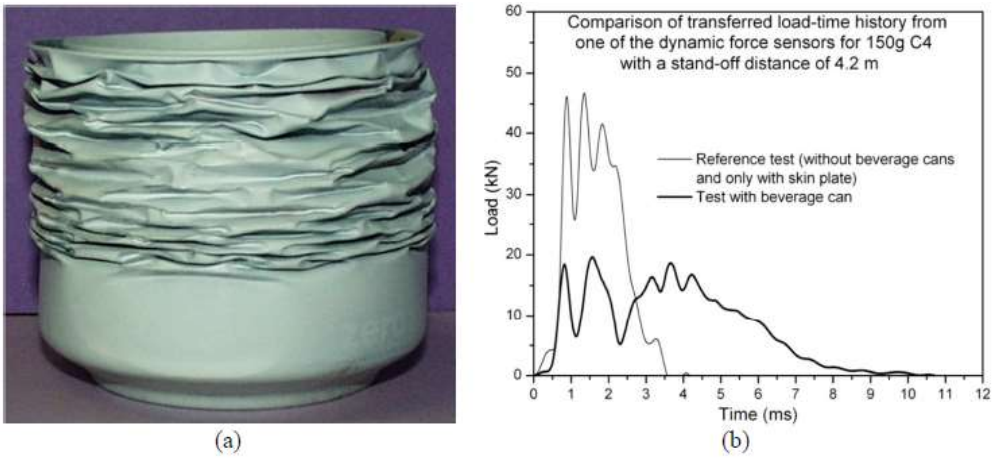

Fig. 2-13 - (a) Example of final deformation pattern of a beverage can. (b) Comparison of transferred load-time histories [6]

From the obtained results, the conclusion is that the beverage cans can be used to protect structures from an air blast load.

In 2015 Lavarnway and Pollino [7] conducted an experimental research about the mitigation of air-blast pressure impulses on buildings. In this study the principles of the conservation of energy was used to assess the application of a blast resistant ductile connector - BRDC, verifying after with a nonlinear finite element and an experimental testing.

The panel tested is a 3,66 m by 7,32 m with 0,15 m thick pre-cast 34,5 MPa concrete panel. This panel is reinforced only for temperature and shrinkage action according to ACI 318-08 [8] and is designed to remain elastic by capacity design to the BRDC. The BRDC is connected to the exterior building frame on top and bottom edges of the panel (Fig. 2-14).

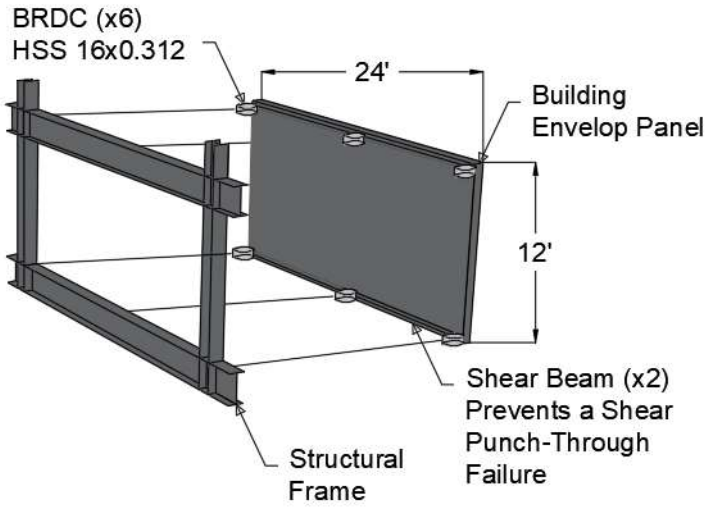

Fig. 2-14 - Implementation of BRDC to building envelope panel [7]

The strength and deformation of this concrete panel was designed to determine the limits on the BRDC for protecting a minimally reinforced panel. The yield strength of the panel will provide an upper limit on the strength of the BRDC (Fig. 2-15).

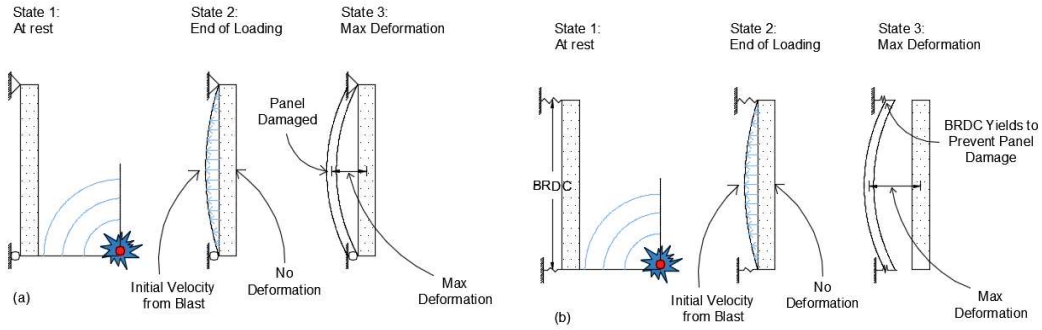

Fig. 2-15 - Illustration of the System Response States (a) without BRDC and (b) with BRDC [7]

A simplified triangular linear function representing the positive phase of the impulse from the blast history is considered instead of the more complex real pressure-time variation (Fig. 2-16). This simplification is considered because it captures the parameters of most interest: the peak reflected pressure (P_r) and the reflected impulse (I_m).

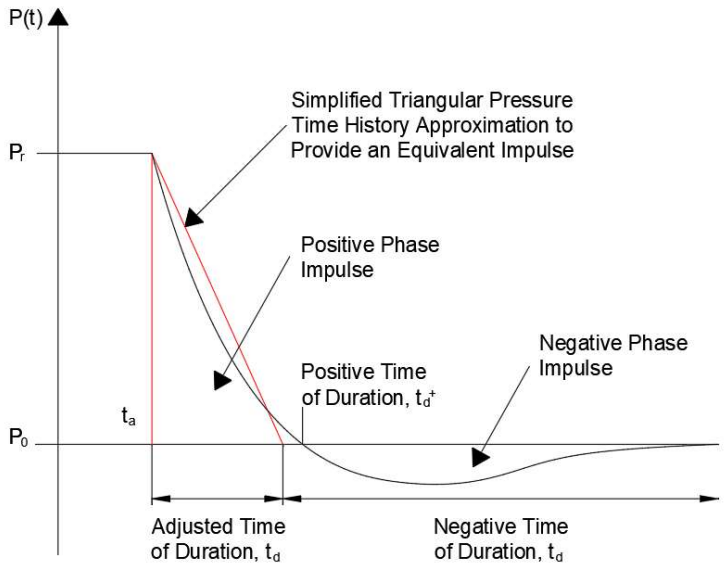

Fig. 2-16 - Free-field pressure-time variation [7]

The relative displacement of the middle and the corner of the panel was calculated and the difference approximately 50 % larger than 4,1 mm, which means that the elastic displacement limit was exceeded. The results of BRDC deformations from the nonlinear transient finite element model and the theoretical model are presented in Table 2-3. The deformation from the nonlinear analysis and from the theoretical evaluation were similar, with an average difference of 9,1%.

The yield forces set to do the tests were set as below 47,6 kN, which is the allowable force for the chosen panel and the lower bound of 13,3 kN. This capacity is so the BRDC yield and deform before the panel yields. These yield forces to BRDC were based in different blast scenarios, with impulses ranging from 100 to 800 kPa*ms.

Table 2-3 - Transient Finite Element Analysis Cases and Results [7]

Case #	Impulse (kPa-ms)	BRDC Yield Force (kN)	FEA Results		Theoretical Model	% Diff, BRDC Disp (Theoretical vs. FEA)
			BRDC Disp (cm)	Dif Panel Def. (mm)	BRDC Disp (cm)	
1	46	46,7	0,44	1,26	0,75	-72,5
2	46	13,4	0,82	0,7	0,97	-17,8
3	140	46,7	1,34	3,86	1,31	2,2
4	140	13,4	2,88	1,51	2,91	-1,0
5	436,2	46,7	6,73	6,55	6,75	-0,2
6	436,2	13,4	21,24	1,98	21,94	-3,3
17	154,9	46,7	1,6	4,55	1,45	9,2
18	154,9	37,8	1,81	4,02	1,64	9,3
19	154,9	13,4	3,77	1,56	3,41	9,5
20	249,4	46,7	3,04	5,28	2,67	12,1
21	249,4	42,3	3,27	4,82	2,89	11,7
22	249,4	13,4	8,59	1,77	7,68	10,6
23	470,1	46,7	8,81	6,61	7,75	12,0
24	470,1	44,9	9,13	6,36	8,03	12,1
25	470,1	31,2	12,76	4,58	11,3	11,5
26	470,1	13,4	27,97	1,99	25,44	9,1
27	95,2	46,7	0,98	2,79	0,98	1,0
28	95,2	42,3	1,04	2,71	1,01	2,5
29	95,2	23,4	1,4	2,02	1,29	7,9
30	95,2	13,4	1,9	1,31	1,74	8,5
31	177,6	46,7	1,9	5,09	1,69	10,6
32	177,6	37,8	2,19	4,26	1,94	11,4
33	177,6	23,4	3,07	2,71	2,72	11,6
34	177,6	13,4	4,83	1,57	4,26	11,9
35	284,9	46,7	3,71	5,48	3,28	12,3
36	284,9	44,9	3,85	5,29	3,39	12,0
37	284,9	13,4	11,17	1,79	9,82	12,1
47	200,2	46,7	2,13	5,06	1,97	7,4
48	200,2	37,8	2,50	4,23	2,28	8,7
49	200,2	13,4	5,91	1,59	5,22	11,6
50	321,0	46,7	4,21	5,48	3,99	5,2
51	321,0	42,3	4,60	5,08	4,34	5,6
52	321,0	13,4	13,74	1,68	12,30	10,5
53	514,4	46,7	9,53	5,84	9,18	3,6
54	514,4	44,9	9,90	5,63	9,52	3,8
55	514,4	33,4	13,46	4,34	12,60	6,4
56	514,4	13,4	33,24	1,78	30,45	8,4

Lavrarnway and Pollino proposed several potential BRDC designs, however they only presented the round hollow structural sections (HSS). A round HSS is expected to dissipate blast energy by plastically deforming radially inward forming four yield lines.

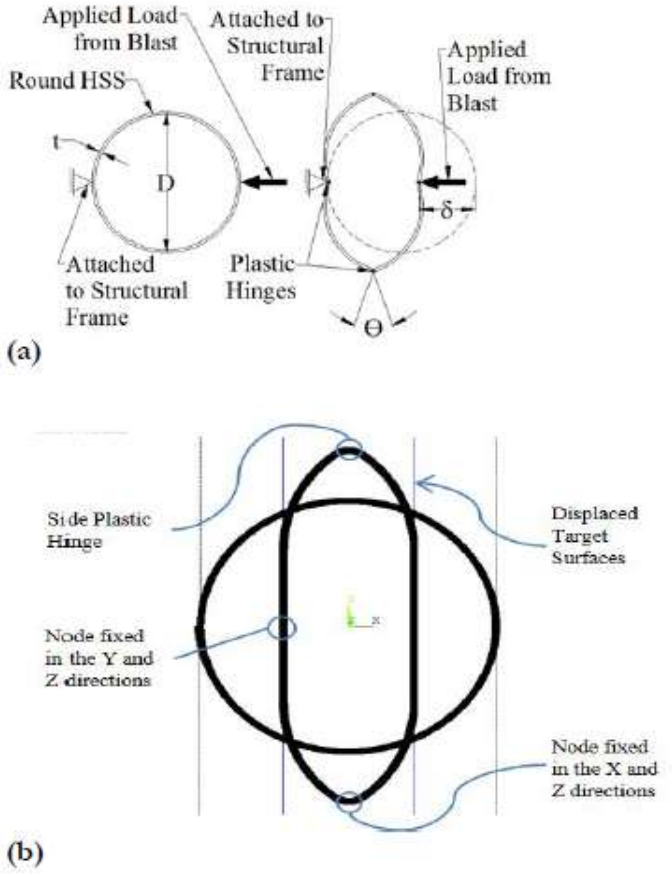

Fig. 2-17 - Potential Loading and Support Conditions for Round HSS

(a) Point Load/Support and (b) Contact Surfaces [7]

The round HSS can be connected to the panel and exterior framing in a configuration that can apply a concentrated line of loads or provides a contact surface at two sides of the HSS as seen in Fig. 2-17.

The plastic compressive capacity of a HSS exposed to a concentrated line of force and response along its dimension can be determined using notions of plasticity and may be evaluated by Eq. (2-1). Different sections and different material grade were tested, as seen in Table 2-4.

Table 2-4 - BRDC Experimental Specimen Details [7]

Section	Steel Grade	Measured yield stress (MPa)	Measures Tensile Stress (MPa)	Measured Thickness (mm)	Section Length Tested (mm)	Exp. Yield Force (kN)	Yield Force (kN)
HSS 16x0.375	A53 Gr. B	380	516	9.78	203	37	36.3
HSS 10.75x0.25	A106 Gr. B	406	477	6.48	203	25	25.3
HSS 7x0.25	A513 Type 5	772	848	6.40	140	44	49.8

The values of the stress-strain for the large displacements expected to develop in the test can be seen in Fig. 2-18. The analysis of the model required the use of the computer program ANSYS, the model was loaded until it reaches the 76 mm displacement required.

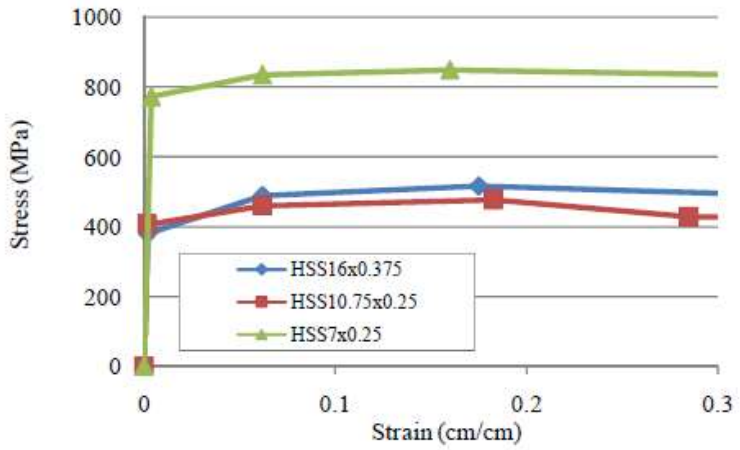

Fig. 2-18 - Stress-strain values used in the Multi-Linear Hardening Material Model [7]

The critical values of the tests can be seen in Table 2-5. The force-deformation and the assessment of the experimental results and the FEA results can be seen in Fig. 2-19.

Table 2-5 - BRDC FEA Results [7]

Section	Stress at Side Hinge (MPa)	Strain as Side Hinge (%)	Yield Force (kN)
HSS 16x0.375	484	5,9	34
HSS 10.75x0.25	476	27,5	25
HSS 7x0.25	853	26,3	45

As expected the stress and strain increases as the diameter decreases. This happens due to the larger rotations that the HSS's with the smaller diameters

must go through because each section is expected to the same 152 mm displacement.

The FEA results and the experimental results show that a HSS provides a very good force and deformation behaviour for the BRDC application considered. The experimental results also showed that if the round HSS experiment cracking at the outer fibres still sustains a good carrying load capacity after the cracking.

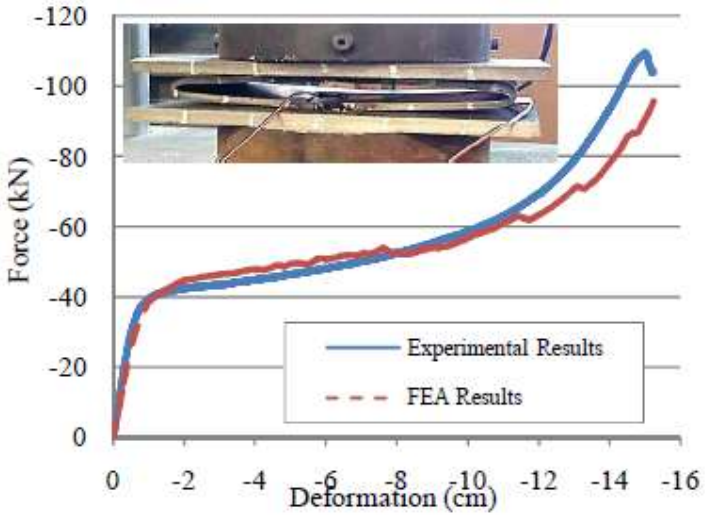

Fig. 2-19 - Force-Deformation Response of a Round HSS7x0.25 and Deformed Configuration at approximately 152 mm [7]

This study shows that the BRDC system can completely dissipate the energy from an explosion without damaging the building. The nonlinear FEA of the BRDC system correlated well with the theoretical results for a large example of practical designs. A round HSS BRDC is the most efficient and provide the performance for the mitigation of blast pressures on a building.

3. ENERGY DISSIPATION DEVICES

3.1. Introduction

To analyse the large-scale models used in this study, the principle of conservation of energy was used. This principle will be explained in the next section. The explosion energy is dissipated mainly by steel hollow circular bars, or tubes, with no welding. The mass, needed for the kinetic energy is given by concrete panels placed on top of the tubes, whose thickness (mass) was designed according to the tube energy dissipation characteristics.

Two types of steel tubes, from ST37 type, were used, one with 2,6 mm of thickness and 48,3 mm external diameter and another with 3,2 mm thickness and with 76,1 mm of external diameter.

The energy dissipation capacity of the tubes was estimated using three models. An analytical model was used considering a plastic behaviour to estimate the tubes plastic deformation energy, which will be explained in section 3.6. A numerical model, using the computer program ADINA, was used to analyse the tubes behaviour and quantify the tubes deformation energy. At last, experimental tests of the tubes were performed, in a compression machine, to quantify the real deformation energy of the tubes.

3.2. Principle of conservation of energy

The energy absorbed by the tubes and the panels can be estimated by using the principle of energy conservation.

$$T = W \tag{3-1}$$

Where T represents the kinetic energy and the W the absorbed energy by deformation of the tubes.

The kinetic energy of a system with one degree of freedom is given by:

$$T = \frac{1}{2} * m_{eq} * v_{eq}^2 \quad \textbf{(3-2)}$$

Where m_{eq} is the equivalent mass and v_{eq} is the equivalent velocity of the system. Therefore, considering the 2º Law of Newton:

$$F = m * a = m * \frac{\Delta \vec{v}}{\Delta t} \quad \textbf{(3-3)}$$

Using the force in the time of interaction:

$$F * \Delta t = m * \Delta \vec{v} \quad \textbf{(3-4)}$$

And knowing that the impulse is:

$$I = F * \Delta t \quad \textbf{(3-5)}$$

Ergo,

$$I = m * \Delta \vec{v} \quad \textbf{(3-6)}$$

So, the kinetic energy can be calculated by:

$$T = \frac{1}{2} * \frac{I_r^2}{m_{eq}} \quad \textbf{(3-7)}$$

The absorbed energy is the area of the graphic force/deformation, which means that the absorbed energy is different in all the methods used in the study. While using a rigid-plastic model, the dissipated energy is obtained as:

$$W = P_p * a_{max} \quad \textbf{(3-8)}$$

Where P_p is the collapse load of the tube and the a_{max} is the maximum deformation.

To estimate the thickness of the concrete panel, it is needed to characterize the explosion. To do this the reflected impulse (i_r), per unit area, can be estimated by:

$$i_r = i_s \frac{P_r}{P_{so}} \tag{3-9}$$

Rankine-Hugoniot [18], according to T. João [9], calculated the reflected overpressure of the peak (P_r) in function of the atmosphere pressure (P_a) and the incident overpressure (P_{so}).

$$P_r = 2P_{so}\left(\frac{7P_a + 4P_{so}}{7P_a + P_{so}}\right) \tag{3-10}$$

Kinney & Graham [9] proposed to estimate the incident overpressure in function of the scaled distance (Z) and the atmosphere pressure (P_a).

$$P_{so} = \frac{808\left[1 + \left(Z/_{4,5}\right)^2\right]P_a}{\sqrt{1 + \left(Z/_{0,048}\right)^2} * \sqrt{1 + \left(Z/_{0,32}\right)^2} * \sqrt{1 + \left(Z/_{1,35}\right)^2}} \tag{3-11}$$

They also propose an empirical equation determining the specific shock wave impulse, per unit area, (i_s).

$$i_s = \frac{0{,}0067\sqrt{1 + \left(Z/_{0,23}\right)^4}}{Z^2 * \sqrt[3]{1 + \left(Z/_{1,55}\right)^2}} \tag{3-12}$$

The scaled distance is a concept usually used to determine the characteristics of the shock wave, this was calculated by Hopkinson & Cranz [10], according to M. Gonçalves [11], using the distance to the centre of the explosion (R) and the equivalent TNT weight of the explosive (W_{TNT}), by the equation:

$$Z = \frac{R}{W_{TNT}^{1/3}} \quad \textbf{(3-13)}$$

3.3. **Steel characterization**

To characterize the steel of the tubes, tensile tests on bone shaped specimens [12] were done in a Zwick machine with the load capacity of 50kN.

The test specimens were cut in the longitudinal direction, knowing that the longitudinal and the transversal directions of the tubes may have different mechanical characteristics, what may have influence on the analysis of the results. Fig. 3-1 shows the test specimens from both 48,3 mm tube and 76,1 mm tube, and Fig. 3-2 shows the dimensions of the specimens. Only three specimens were tested for each tube diameter.

Fig. 3-1 - Test pieces from 48,3 mm and 76,1 mm

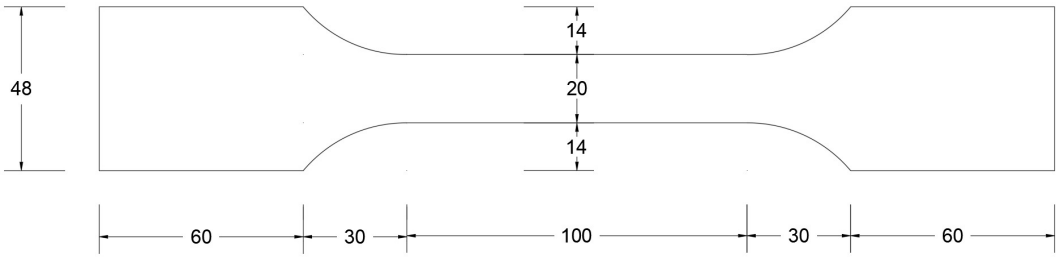

Fig. 3-2 - Dimensions of the test specimens

Fig. 3-3 shows the behaviour of the steel specimens under tension and the average values of the yielding stress (f_y), the elastic modulus (E_s), the maximum stress (f_t) and the strain hardening modulus (E_p), calculated by using a point in the beginning of the plastic phase and another in the end, in Table 3-1.

Table 3-1 - Steel characteristics

Ø (mm)	f_y (MPa)	E_s (GPa)	f_t (MPa)	E_p (MPa)
48,3	453	180	585	1445
76,1	452	217	528	673

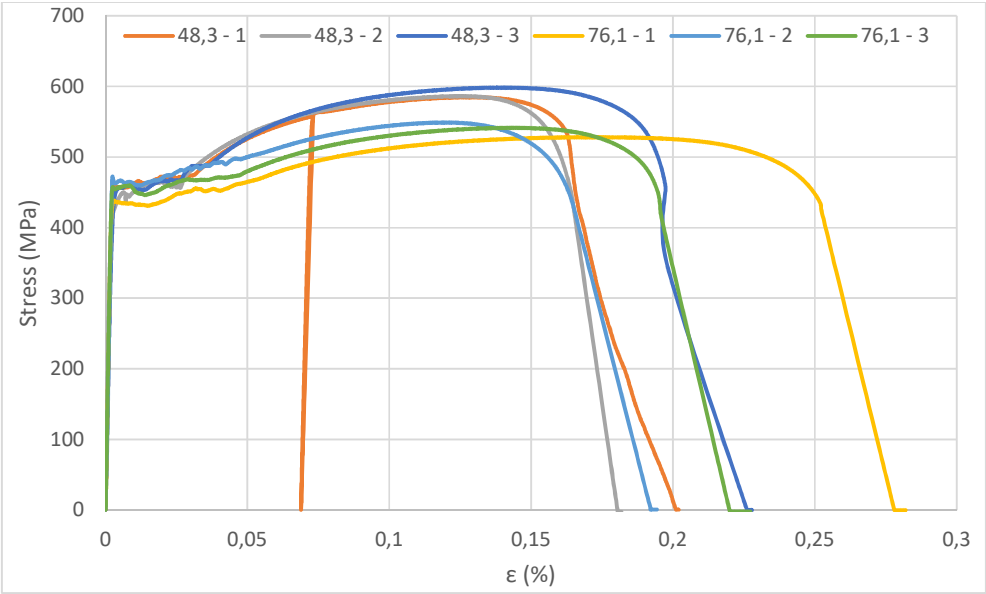

Fig. 3-3 - Results of the tensile test to the tubes of 48,3 mm and 76,1 mm

3.4. **Experimental tests of the tubes under compression**

The tube specimens were tested in a Zwick machine with the load capacity of 50kN. The test results will be used to calibrate the numerical and analytical models. From these tests the energy dissipation of the tubes and other mechanical characteristics are obtained. To simulate the real situation where the tubes were compressed between two steel plates, Fig. 3-4. Three specimens, with 150 mm long, of each tube diameter were tested. The test results are shown in Fig. 3-5.

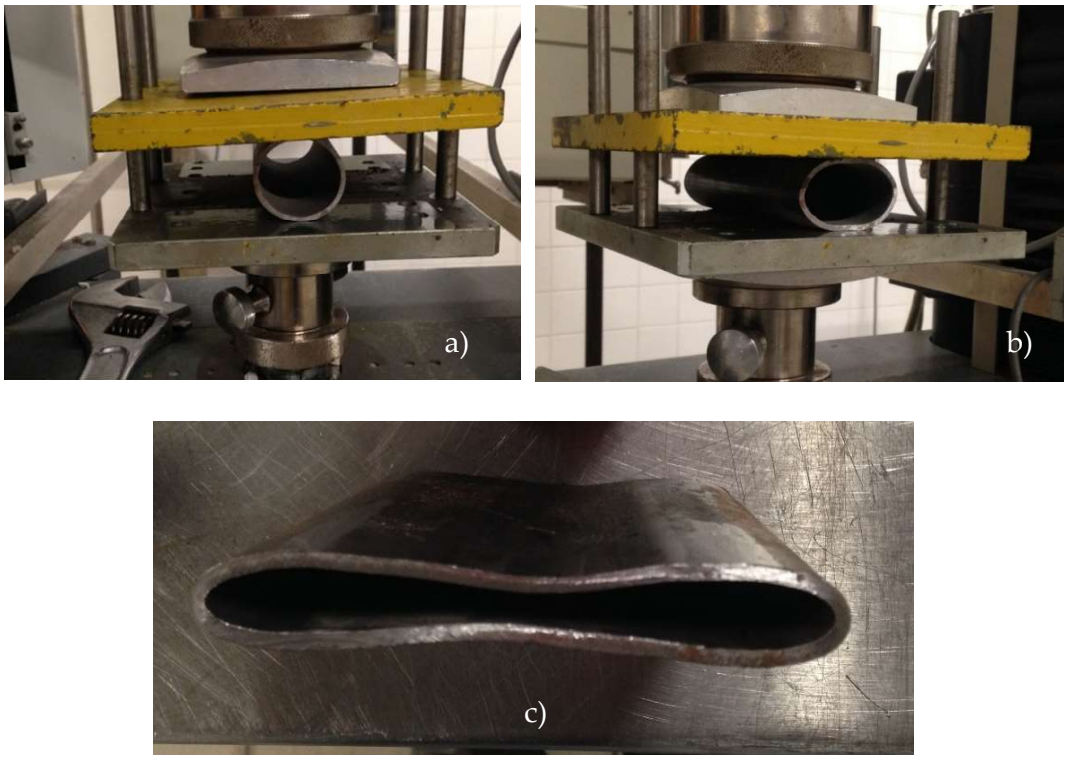

Fig. 3-4 – Sequence of the compression test a) tube before suffers any deformation; b) tube while being deformed; c) tube totally deformed

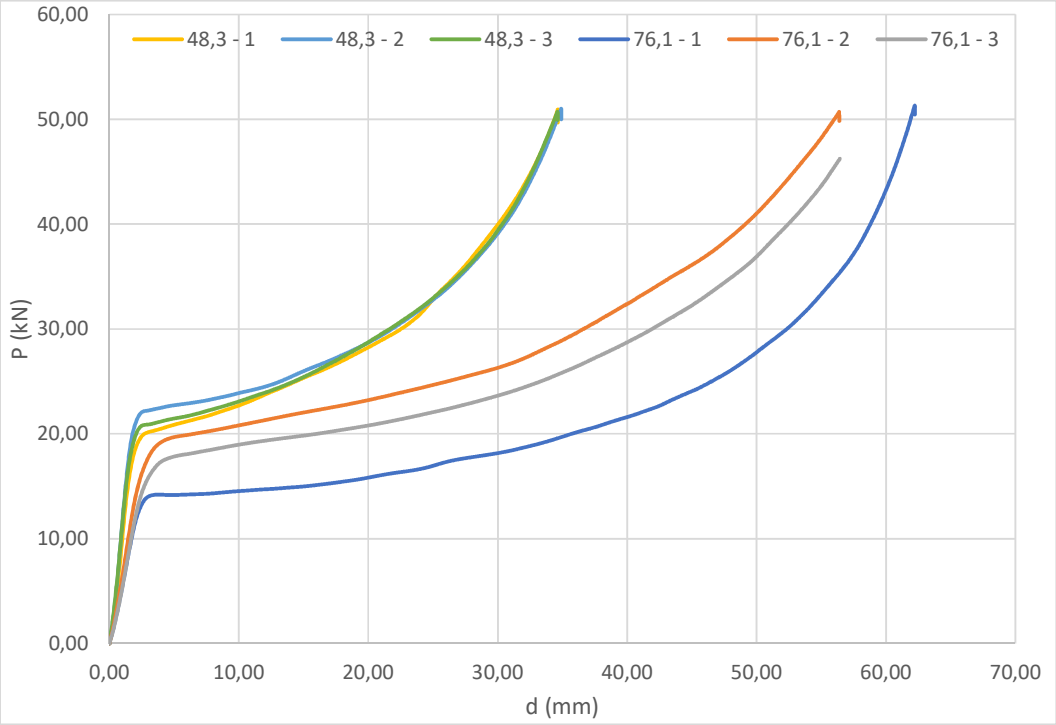

Fig. 3-5 - Results of the compression test on the tubes of 48,3 mm and 78,3 mm diameter

Table 3-2 - Yielding forces from the tubes compression tests

Ø (mm)	**P_y (kN)**	**$P_{y,av}$ (kN)**
48,3	19,46	20,58
	20,56	
	21,72	
76,1	13,81	16,66
	19,21	
	16,97	

3.5. **Numerical model**

The numerical model was developed using the finite element program ADINA. ADINA was used to perform a nonlinear analysis and considering material non-linearities and large deformations, to understand the tube behaviour under

increasing transversal force. This program allows to export the force-deformation data, so the dissipated energy can be calculated.

Fig. 3-6 shows only one-quarter of the tube to reduce the calculation effort. With only a quarter of the tube modelled, the deformations and the force are half the real ones. The ends of the model were only allowed to move in one direction with no rotation, as it can be seen in Fig. 3-6, so the end C could only move vertically and the edge B could only move horizontally. Fig. 3-7 shows the force/displacement plot obtained from this analysis.

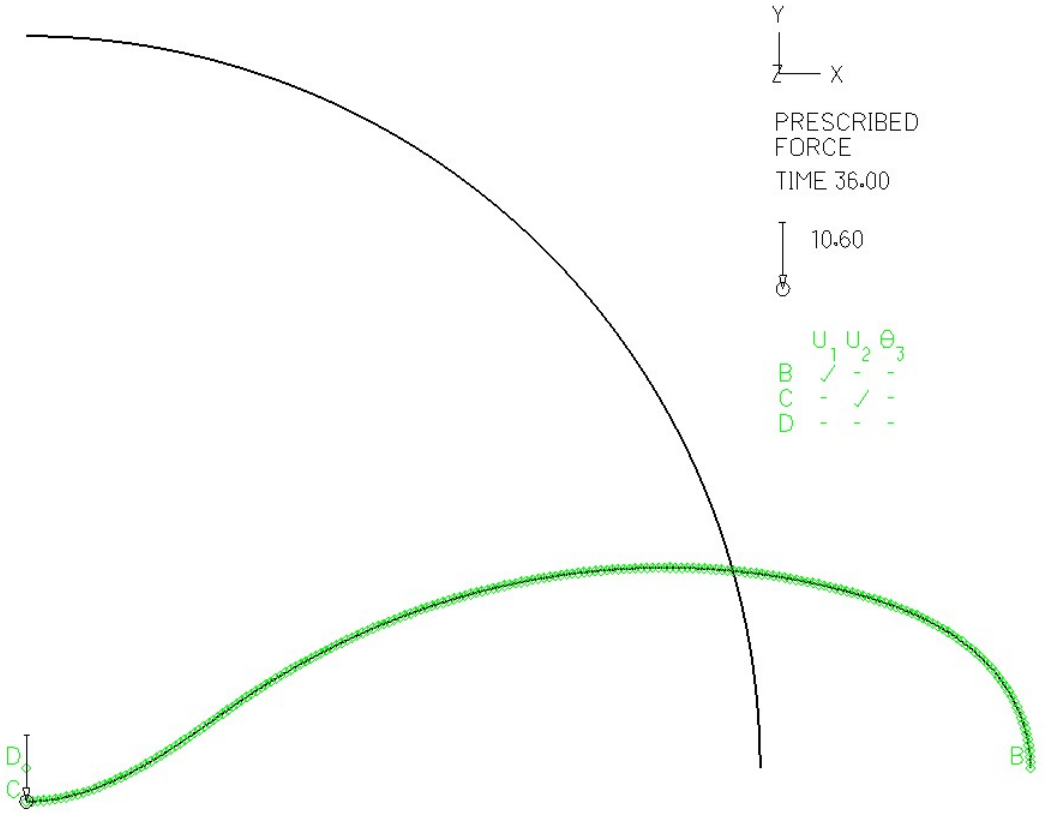

Fig. 3-6 - Finite Element mesh and the deformed of the ADINA model

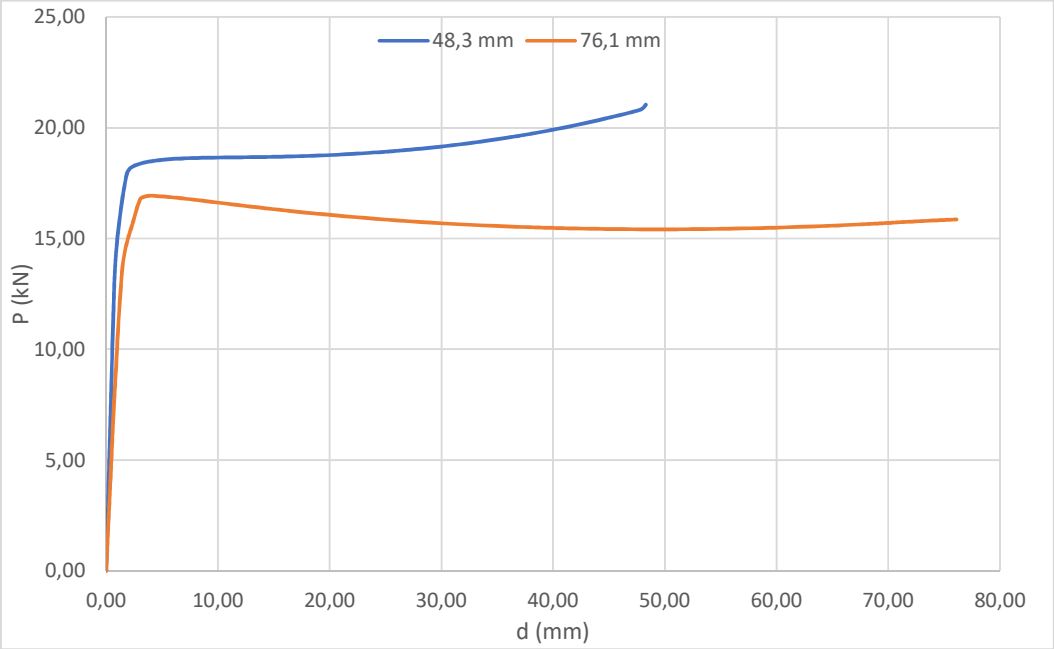

Fig. 3-7 - Force/displacement graphic from ADINA

Comparing the Fig. 3-7 with Fig. 3-10 the differences can be seen, this happens because in ADINA it was not considered the drifting of the force when the deformation is occurring, this means that in the plastic zone of the graphic the force does not grow as it grows in the analytical model presented in the next chapter.

3.6. **Analytical model**

The analytical model was made using a plastic model. The tubes are compressed between plates and it is assumed that the tubes plasticize in four plastic hinges, Fig. 3-8, and assuming, as well, that there is no deformation between the plastic hinges, i.e., rigid bodies were considered between these plastic hinges. Eq. (3-14) may be obtained by equilibrium of the model shown in Fig. 3-8. The distance *d*, between the force application point and the mid-height plastic hinge, may be obtained from Fig. 3-8, reduced by the dimension of the mid-height plastic hinge, that was assumed equal to the thickness of the tube wall.

$$P_p \times d = 2 \times M_p \quad \textbf{(3-14)}$$

$$d = \frac{\sqrt{D^2 - a^2}}{4} - t \quad \textbf{(3-15)}$$

In these equations P_p stands for the applied plastic force, M_p is the plastic moment of the tube wall, D is the tube diameter at the centre of the wall (exterior diameter minus the wall thickness), and a is the tube transversal deformation.

In the case of no deformation, the force is applied on the top of the tube. As the deformation grows the force position moves and the horizontal distance (d) decreases, between the force application point and the mid-height plastic hinge, as it can be seen in Fig. 3-8.

Considering a moment linear variation from M_y to M_p the values obtained by Eq. (3-14) were multiplied by a coefficient k, resulting in Eq. (3-17), which varies between 1 and M_p/M_y accordingly to Eq. (3-16), where a is the deformation of the tube and $(D\text{-}t)$ the maximum deformation the tube can withstand. This moment variation from M_y to M_p is due to the change of the stress distribution in the wall cross section and due to the strain hardening of the steel.

$$k = 1 + \left(\frac{M_p}{M_y} - 1\right) \times \frac{a}{D - t} \quad \textbf{(3-16)}$$

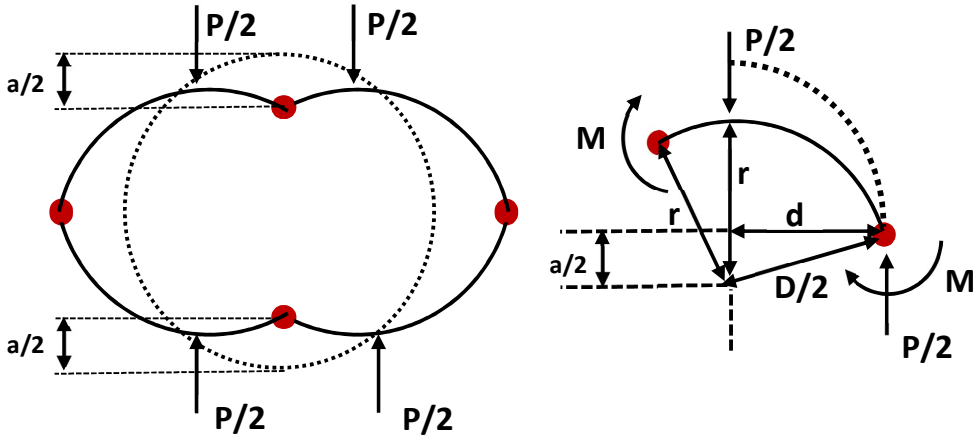

Fig. 3-8 - Mechanism used to calculate the analytical model

$$P = \frac{8 \times M_y}{\sqrt{D^2 - a^2} - 4 * t} \times k \tag{3-17}$$

The yielding moment M_y and the ultimate moment M_p may be determined by Eq. (3-18) and (3-19), where b is the length of the tube, i.e., the width of the tube wall cross section, t is the thickness of the tube wall (see), f_y is the yield steel stress and f_t is the ultimate steel stress. Note that, to simplify the analysis, the axial force in the mid-height plastic hinge was not considered in the quantification of the yielding moment and the ultimate moment.

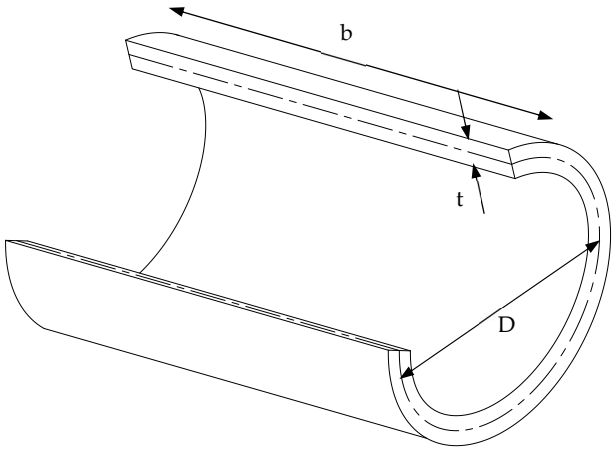

Fig. 3-9 - Dimension of the steel tube

$$M_y = f_y * \frac{b * t^2}{6} \quad \textbf{(3-18)}$$

$$M_p = f_t * \frac{b * t^2}{4} \quad \textbf{(3-19)}$$

As can be seen in Fig. 3-10, while using this model, the force *P* rises with the tube transversal deformation, because the distance *a* between the application point of the force and the mid-height plastic hinge decreases, and due to the *k* factor described above.

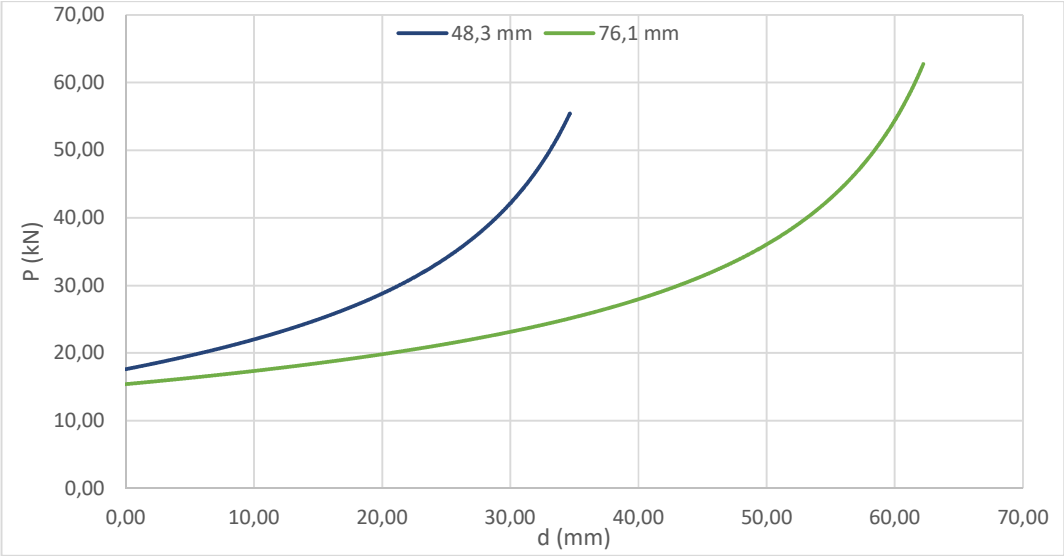

Fig. 3-10 – Force/displacement graphic for the plastic model

Taking into account the steel characteristics obtained in the tensile tests, Table 3-3, presents the values that, while using this analytical model, represents the behaviour of the tubes under compression.

Table 3-3 - Representative values of the analytical model

Ø (mm)	**M_y (kNm)**	**M_p (kNm)**	**$k_{max} = M_p / M_y$**	**P(d=0) (kN)**
48,3	76,56	149,57	1,95	17,35
76,1	115,71	207,36	1,79	15,40

3.7. **Analysis of the results**

Fig. 3-11 and Fig. 3-12 show the force/displacement plot of the tests of three 48,3 mm and 76,1 mm diameter tubes, respectively. The results obtained show that the analytical model is closer than the ADINA model to the test results. The figures also show that the ADINA model adjusts quite well in the elastic phase, in the plastic phase the model does not contemplate the drift of the force while the deformation occurs. Both models do not have the same yielding force point as in the real tests, this shows the difference in the transversal and the longitudinal directions of the steel.

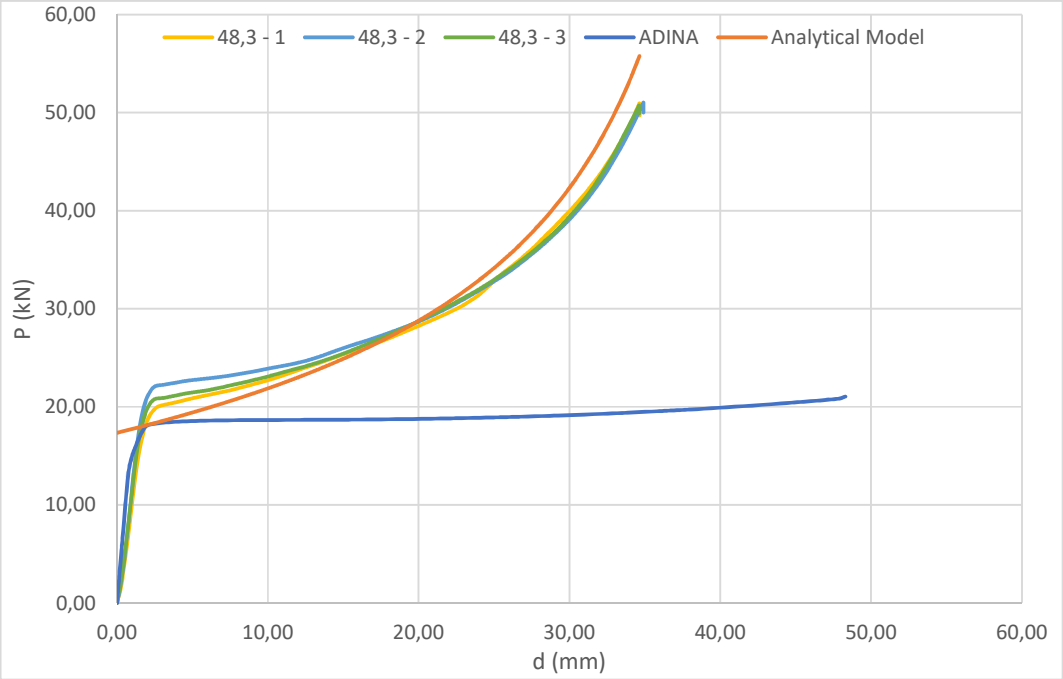

Fig. 3-11 – Comparison from the laboratorial, analytical and ADINA for 48,3 mm tube

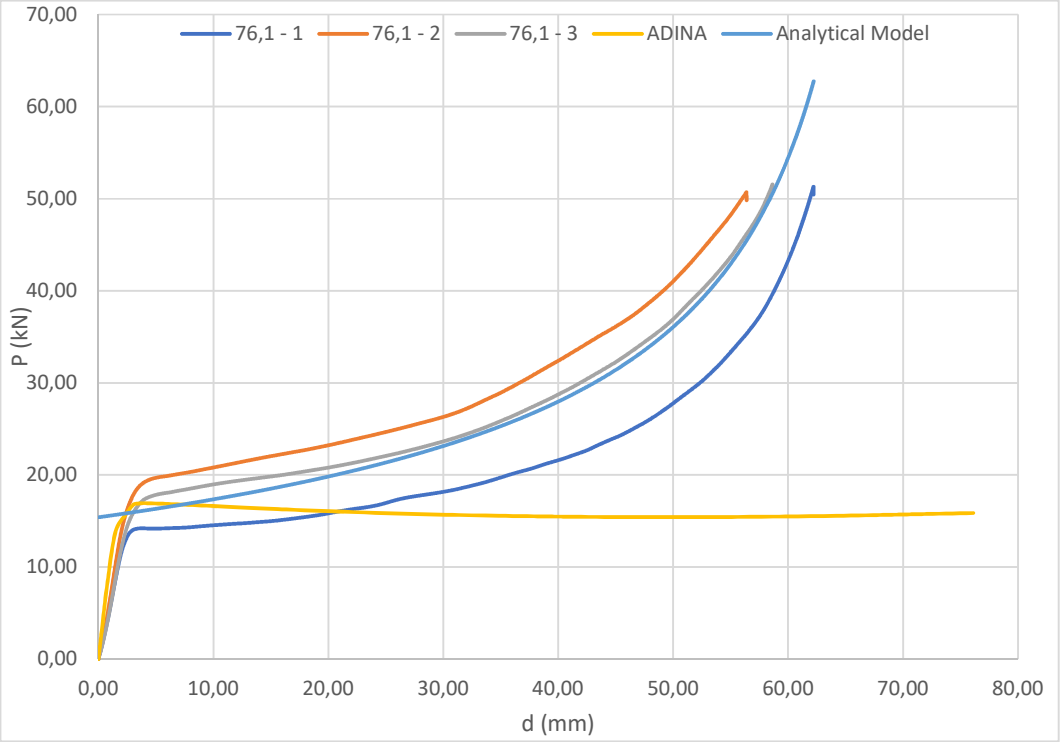

Fig. 3-12 - Comparison from the laboratorial, analytical and ADINA for 76,1 mm tube

4. TEST OF LARGE SCALE MODELS

4.1. Introduction

The aim of these experimental research was to study a solution of steel tubes, distributed over a concrete slab and supporting concrete plates with a predefined thickness. The mass of the concrete plates, with a pre-established thickness, would define a kinetic energy that the plastic deformation of the steel tubes would dissipate. The base slab reinforcement was designed to resist the maximum plastic force of the dissipaters without yielding.

The objectives of the research were not achieved because there were two mistakes in the production of the testing models. The precast contractor did not supply top plates with the designed thickness (two different thickness were specified: 0,06 m and 0,10 m) and the plates supplied were only 0,07 m thick. On the other hand, the bottom reinforced concrete slabs had the bottom reinforcement on the top face and a much weaker reinforcement on the bottom. This last error was only detected after the tests.

The aim was to analyse two parameters in this study: different masses of the top concrete panels, corresponding to two different panel thicknesses; and different energy dissipaters, corresponding to two different steel tubes (76,1 mm diameter with 3,2 mm wall thickness and 48,3 mm diameter with 2,6 mm wall thickness).

The present chapter describes the tested models.

Initially, it was planned to test four models: one slab alone, to be considered as the reference model; one model with 0,10 m thick plates and 76,1 mm diameter steel tubes; one model with 0,06 m thick plates and 76,1 mm diameter steel tubes; and one model with 0,06 m thick plates and 48,3 mm diameter steel tubes. Considering that only 0,07 m thick plates were supplied, the following

tests were performed: one slab alone, reference model; one model with 0,07 m thick plates and 76,1 mm diameter steel tubes; and one model with 0,07 m thick plates and 48,3 mm diameter steel tubes.

The blast tests campaign was performed at the Campo Militar de Santa Margarida. The handling and transportation of all the explosive material were done by the army personnel and in agreement with the security procedures approved by the Portuguese Army.

4.2. **Experimental Models**

In order to test the anti-blast system, four reinforced concrete pre-cast slabs were used, with 2,6 x 2,0 m and 0,12 m thick. One slab was the reference specimen and the other two had different dissipating systems:

- 8 panels with 0,07 m on top of 32 steel tubes of 76,1 mm external diameter;
- 8 panels with 0,07 m on top of 32 steel tubes of 48,3 mm external diameter

The concrete slab was drilled to fix the steel tubes. Three holes were done per line of tubes (Fig. 4-1). The tubes were fixed with interlaced wire.

Fig. 4-1 - Worker drilling a slab

Fig. 4-2 shows the layout of the steel tubes and at the upper concrete panels. Each line had four tubes 0,350 m away from each other, in 8 lines 0,325 m apart. Each 0,07 m thick panels were placed on top of four steel tubes.

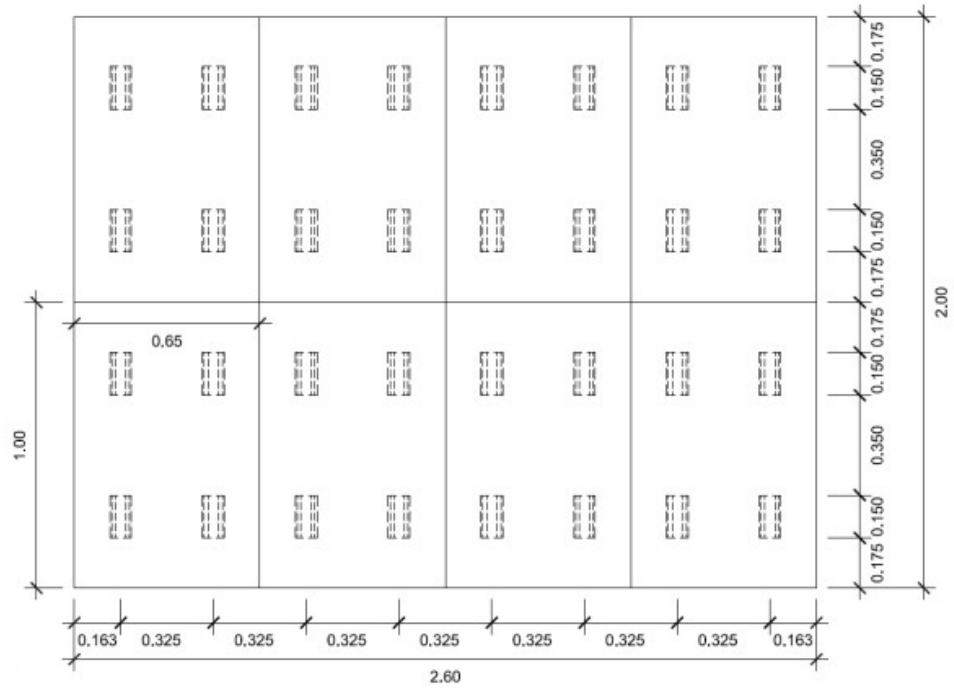

Fig. 4-2 - Layout of the steel tubes and the upper panels

The three bottom slabs are reinforced with a ϕ5//0,10 on the bottom, as may be seen in Fig. 4-4, and ϕ10//0,10 on top. Fig. 4-3 shows the casting of the bottom slab, at Concremat, with the mentioned steel reinforcement.

Fig. 4-3 - Casting of the bottom slab

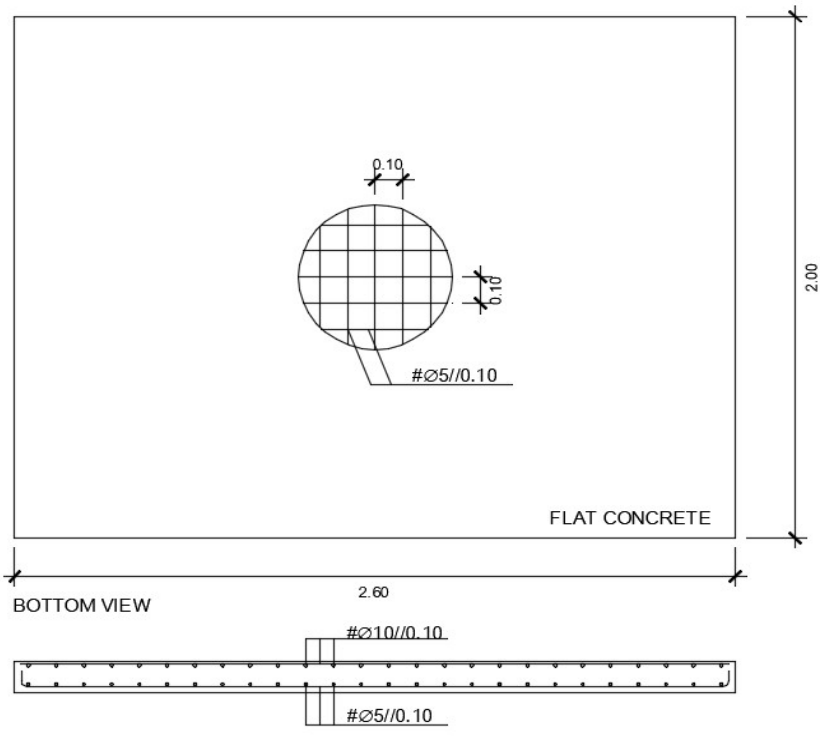

Fig. 4-4 - Bottom view of the concrete slab with reinforcement

The concrete cubes were tested under compression the day after the test of the models, the results are presented in section 4.5.

The upper concrete panels are 1,00 m x 0,65 m, with 0,07 m thickness and these panels are reinforced with an electro-welded welsh #NAQ50, which is squared mesh with bars ϕ5 spaced 0,10 m.

The two types of steel tubes chosen, 76,1 mm and 48,3 mm (Fig. 4-5), have different energy dissipation capacity due to different yielding force and maximum displacement

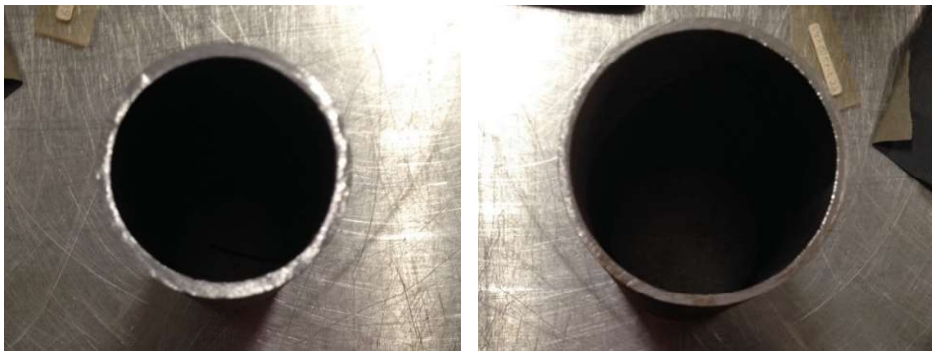

Fig. 4-5 - 48,3 mm and 76,1 mm tubes

The steel tubes distribution is presented in Fig. 4-2 and the assembly of the slab with the tubes can be seen in Fig. 4-6.

Fig. 4-6 - Slab with 48,3 mm steel tubes assembled

4.3. **Testing System**

The system was composed by four inverted T beams, with 0,30 m in height and 1,65 m long, where the models were supported.

The explosive was mounted in a gallows structure, to ensure that the height of the explosives was the correct one and tighten by strands to anchor in the ground to be sure that the explosive didn't move due to the wind force. Fig. 4-7 is shown the system described. This system ensures that there's no obstacle between the explosives and the model, i.e., the shock wave doesn't have amplifications due to reflection.

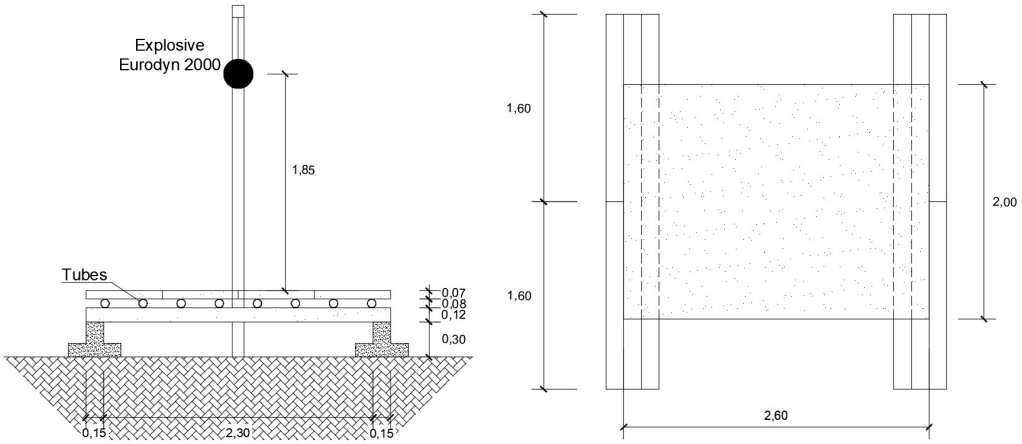

Fig. 4-7 - Scheme of the testing system

The explosive was Eurodyn 2000 (Fig. 4-8) which is a type of dynamite with a base of nitroglycol, offered by ORICA Mining Services Portugal. The explosives were mounted in 50 cylindrical cartridges of 120 g each, to reaches 6,0 kg. Eurodyn 2000 explosive has an equivalent weight to TNT of about 75%, resulting in a W_{TNT} = 4,5 kg.

Fig. 4-8 - 6 kg of Eurodyn 2000

The explosives were mounted at 1,85 m (Fig. 4-9) from the top of the slab.

Fig. 4-9 - Gallows structure to position the explosive

Considering these parameters, the shock wave can be characterized (see section 3.2) by the parameters shown in Table 4-1.

Table 4-1 - Explosion characteristics

P_a (Pa)	Z (m/Kg$^{1/3}$)	P_{so} (MPa)	P_r (MPa)	I_s (MPa.s)	i_r (MPa.s)	$I_{r,\ total}$
101325	1,12	0,79	4,05	0,11	0,57	2,95

After the test, the residual and the instantaneous deflection at mid span as well as the cracks formed by bending of the slab, were measured.

For the residual deflection at the mid-span, a two meter straight aluminium profile and a measuring tape were used (Fig. 4-10). The deformation of the slab was also measured before the explosion to know exactly which was the residual deformation of the slab due to the blast

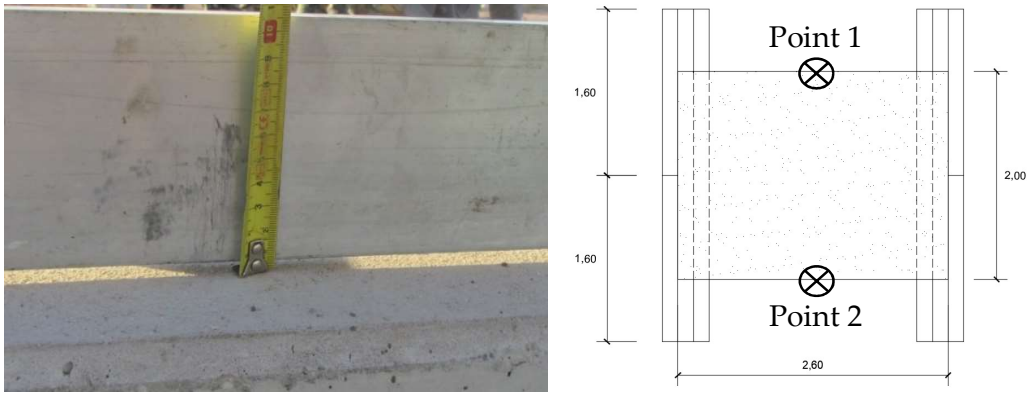

Fig. 4-10 – Measurements of the residual deformation of the slab

To measure the instantaneous deflections, the system used consisted on two blocks of wood laying with five holes (Fig. 4-11), which were filled in with an expansive foam. A rod with 170 mm was inserted partially in each foam box, allowing for about 150 mm to drop out and mark the instantaneous deflections. The instantaneous deformations suffered by the slab are known measuring the difference between the depth marked before the explosion and the new depth of the rods.

Fig. 4-11 - Measuring system for the instantaneous deflection of the model

4.4. **Test results**

Table 4-2 summarizes the characteristics of the four models tested. In this table h_1 stands for the thickness of the top concrete plates, h_2 is the thickness of the bottom slab and ϕ is the steel tubes external diameter.

Table 4-2 – Tested large scale models

Test	W_{TNT} (Kg)	Z (m/Kg$^{1/3}$)	h_1 (m)	h_2 (m)	∅ (mm)
FS1	4,5	1,12	–	0,12	–
FS2	4,5	1,12	0,07	0,12	76,1
FS3	4,5	1,12	0,07	0,12	48,3
FS4	4,5	1,12	–	0,12	–

- Test of model FS1:

In this test the slab got several cracks in the bottom surface. Crack openings up to 0,25 mm (Fig. 4-12) were measured in the slab edges and up to 0,30 mm were measured in the bottom surface (Fig. 4-13)

Fig. 4-12 – Model FS1 - Cracking on the edge of the slab

The instantaneous deflection measured by the system described shown values between 10 mm and 25 mm. Some rods of the measuring device could not be read due to a failure in the foam because some of the foam was not in the best conditions.

Fig. 4-13 – Model FS1 - Cracks on the bottom surface of the slab

The residual deformation was measured in two points and the values were 6 mm and 10 mm, respectively.

- Test of model FS2:

The second test (Fig. 4-14), the plastic deformation of the steel tubes is quite visible (Fig. 4-15). The maximum residual deformation was 18 mm for the tubes in the centre of the slab.

Fig. 4-14 – Model FS2 - prepared to be tested

Fig. 4-15 - Model FS2 - Deformation on the steel tubes

Although the tubes had large deformations, the lower slab also had some cracks (Fig. 4-16), but not as big as in the reference slab. As explained before, the system was not designed to have such cracking in the reinforced concrete slab. Cracks with openings between 0,05 mm to 0,15 mm go all the way through the centre of the slab, due to bending. The slab also had cracks on the corners which mean that the slab wasn't supported equally along the two edges.

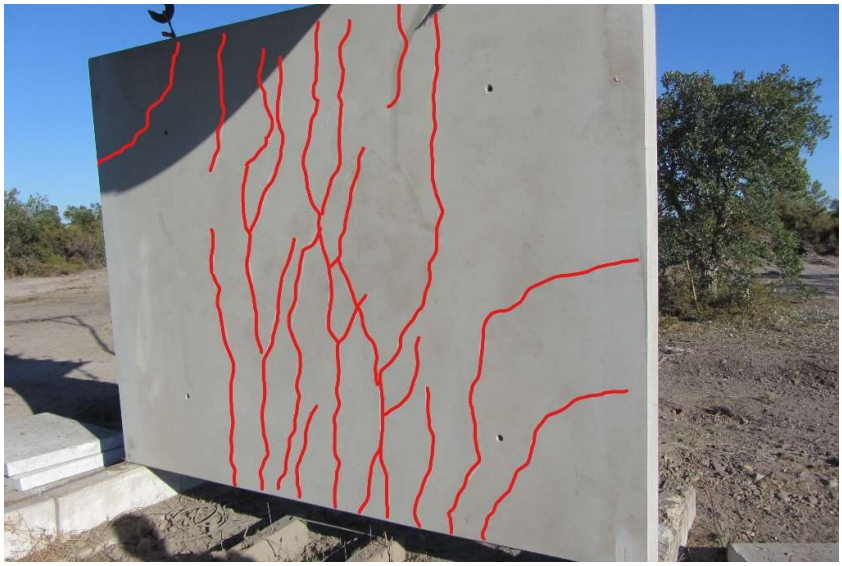

Fig. 4-16 - Model FS2 - Cracks in the bottom surface of the slab

The residual and the instantaneous deformations were smaller than on the first slab, as it can be seen in Table 4-3

- Test of model FS3:

The third test (Fig. 4-17) the deformation of the steel tubes was smaller than in the previous one. The largest deformations were in the steel tubes placed in the centre of the slab, where deformations of around 4,5 mm were measured (Fig. 4-18).

Fig. 4-17 - Model FS3 ready to test

Fig. 4-18 - Model FS3 - Deformed tubes

As in the previous tests, the bottom surface of the slab had cracks, along all the slab, due to bending (Fig. 4-19). These cracks are wider than in model FS2 and vary from 0,05 mm to 0,20 mm, what is also an improvement in relation to the reference model. However, the instantaneous and residual deformations were smaller than in model FS2, as can be seen in Table 4-3

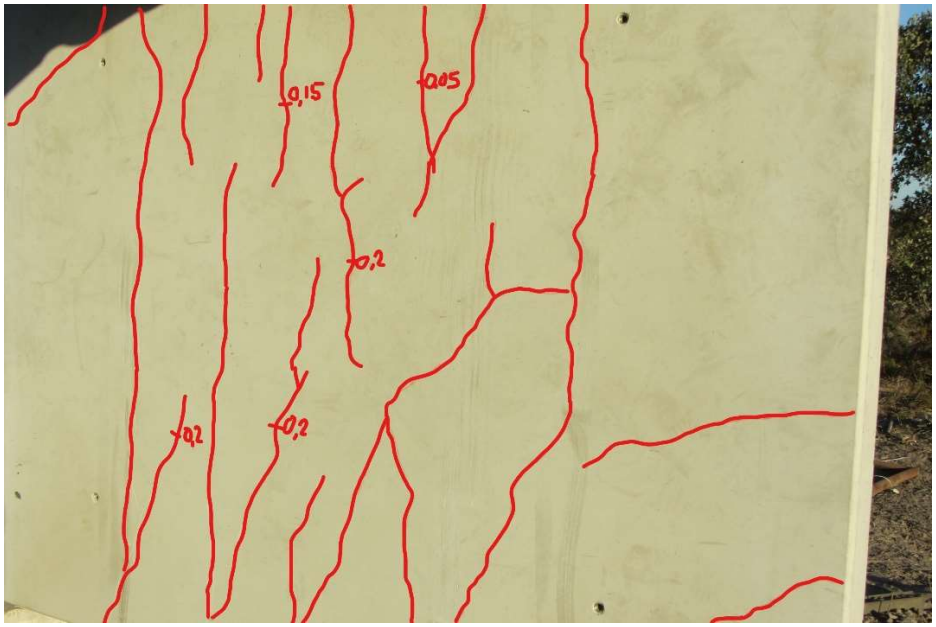

Fig. 4-19 - Model FS3 - Cracks on the bottom surface of the slab

- Test of model FS4:

As in the first reference slab tested this also got numerous cracks in the bottom and on the edge of the slab. These cracks are in the order of 0,15 mm, and 0,1 mm in the edge of the slab (Fig. 4-20).

Fig. 4-20 - Cracks on the bottom and on the edge of the slab

The measured instantaneous deformation was around 14 and 25 mm. The residual deformation was 7 and 8 in the two points measured. These results are in the same region as in the first reference slab, this can be seen in Table 4-3.

Table 4-3 - Deformations of the slab models

Experimental model	Measured deflections (mm)		
	Instantaneous	Residual	
FS1	10 to 25	6	10
FS2	30 to 40	7	4
FS3	16 to 29	5	5
FS4	14 to 25	7	8

4.5. Concrete characterization

The concrete utilized in this study was delivered by Concremat Lda, with the concrete slabs there were, also, provided the respective cubes of each concrete slab. The compression tests of the cubes were performed in the Civil Engineering department laboratory of the FCT – UNL.

The compression resistance of the concrete determined with the test of 16 cubes, with 150 mm edge, cast on 21, 22 and 23 of June, (Fig. 4-21). The tests were performed at October the 2nd, one day after the large-scale tests in Sta. Margarida, that took place in October the 1st.

Fig. 4-21 - Cube testes in the laboratorial of the civil department of FCT-UNL

In Table 4-4 the results of these compression tests can be seen.

Table 4-4 - Results of the compression tests

	21-06-2017			22-06-2017			23-06-2017		
	Weight (Kg)	**Force (kN)**	**Stress (MPa)**	**Weight (Kg)**	**Force (kN)**	**Stress (MPa)**	**Weight (Kg)**	**Force (kN)**	**Stress (MPa)**
1	7,880	1291	57,4	7,845	1213	53,9	7,935	1295	57,6
2	7,930	1260	56,0	7,865	1245	55,3	8,020	1198	53,2
3	7,800	1270	56,4	7,870	1282	57,0	7,935	1251	55,6
4	7,840	1275	56,7	7,935	1258	55,9	7,990	1167	51,9
5	-	-	-	7,865	1338	59,5	7,830	1227	54,5
6	-	-	-	8,050	1266	56,3	7,955	1283	57,0

The value that will be used for the calculations is the average stress $f_{cm,cube}$ which is 55,9 MPa, with this value it is possible to calculate the average compression

stress for a cylindrical samples (f_{cm}), to do this it was considered the following expression and not the expression presented in the EC2 [13], because from the numerous tests done as been confirmed that the average stress is near 90 % of the compression stress from the cubes, instead of the 80 % from the EC2 [13].

$$f_{cm} = 0{,}9 * f_{cm,cube} = 50{,}3\ MPa \quad \textbf{(4-1)}$$

With f_{cm} the characteristic stress (f_{ck}) of the concrete can be calculated also presented in EC2.

$$f_{ck} = f_{cm} - 8 = 42{,}3\ MPa \quad \textbf{(4-2)}$$

With these two characteristics it is possible to know the average tensile stress (f_{ctm}) and the young modulus of the concrete (E_{cm}) with the expressions in the EC2.

$$f_{ctm} = 0{,}3 * f_{ck}^{2/3} = 3{,}6\ MPa \quad \textbf{(4-3)}$$

$$E_{cm} = 22 * \left(\frac{f_{cm}}{10}\right)^{0{,}3} = 35{,}7\ GPa \quad \textbf{(4-4)}$$

5. ANALYSIS OF THE RESULTS

5.1. **Blast action**

The principles presented in section 3.2 were used to analyse the shock wave of the explosion effects on the large scale models.

The first step to characterize the shock wave is the scaled distance, this can be done through Eq. (3-13). Eurodyn 2000, the used explosive, has 75% of the power of TNT, which means that the 6 Kg of Eurodyn 2000 used corresponds to 4,5 Kg of TNT.

$$Z = \frac{R}{W_{TNT}^{1/3}} = \frac{1{,}85}{4{,}5^{1/3}} = 1{,}12\ m/kg^{1/3}$$

With this value of *Z*, when the shock wave hits the slabs it will not be plane once this value is below 1,5 $m/kg^{1/3}$ according to Nabais [14]. For simplification the shock wave will be described as a distributed impulse throughout the surface of each slab.

After knowing the scaled distance, it can be defined the peak pressure (P_{so}) and the specific positive impulse (i_s), using Eq. (3-11) and Eq. (3-12) respectively. These analytical equations, from Kinney and Graham [9], were chosen over the abacus of the American standard [15] once the results are very similar.

$$P_{so} = \frac{808 * \left[1 + \left(\frac{Z}{4{,}5}\right)^2\right] * P_a}{\sqrt{1 + \left(\frac{Z}{0{,}048}\right)^2} * \sqrt{1 + \left(\frac{Z}{0{,}32}\right)^2} * \sqrt{1 + \left(\frac{Z}{1{,}35}\right)^2}} = 0{,}79\ MPa$$

$$i_s = \frac{0{,}0067\sqrt{1 + \left(Z/_{0{,}23}\right)^4}}{Z^2 * \sqrt[3]{1 + \left(Z/_{1{,}55}\right)^2}} = 0{,}11\ MPa * ms$$

Having the value of the peak pressure the reflected pressure peak (P_r) can be calculated through Eq. (3-10), using the value of atmospheric pressure (P_a) of 1,01 MPa.

$$P_r = 2P_{so}\left(\frac{7P_a + 4P_{so}}{7P_a + P_{so}}\right) = 4{,}05\ MPa$$

Lastly, the specific reflected impulse (i_r) can be calculated from Eq. (3-9).

$$i_r = i_s \frac{P_r}{P_{so}} = 0{,}57\ MPa * s$$

Other aspects that should be taken in consideration for the characterisation of the shock wave are the duration of the positive shock wave (t_0), according to Kinney and Graham [9].

$$t_0 = W_{TNT}^{1/3} * \frac{980 * \left(1 + \left(\frac{Z}{0{,}54}\right)^{10}\right)}{\left(1 + \left(\frac{Z}{0{,}02}\right)^{3}\right) * \left(1 + \left(\frac{Z}{0{,}74}\right)^{6}\right) * \sqrt{1 + \left(\frac{Z}{6{,}9}\right)^{2}}} = 1{,}03\ m \qquad \textbf{(5-1)}$$

The velocity of the wave (U) is another important aspect to describe the shock wave, the next equation was suggested by Rankine-Hugoniot [18].

$$\mathrm{U} = C_o * \sqrt{1 + \frac{6 * P_{so}}{7 * P_a}} = 0{,}99\ m/s \qquad \textbf{(5-2)}$$

Having (C_0) as the velocity of the propagation of the sound through the air with 340,29 *m/s*, and the two temperatures (T and T_0) in degrees Kelvin. In the tests the temperature considered was (T) is 303,15 Kelvin and (T_0) is 273,15 Kelvin.

The wave length (L_w) is the region that the pressure of the shock wave is higher than the atmospheric pressure.

$$L_w = \mathrm{U} * t_o = 1{,}00\ m \quad \textbf{(5-3)}$$

5.2. **Expected behaviour of the models**

In this section, the expected behaviour of the designed proposed system is analysed. The slab will be analysed taking into consideration that the bottom reinforcement is ϕ10//0,10. The tubes considered in this section will be one type of tube, steel S235, with two different diameters, 48,3 mm and 76,1 mm both with 2,6 mm of wall thickness.

5.2.1. Dynamic materials behaviour

An explosion is a dynamic action, which means that the concrete resistance and the steel yielding stress need to be affected by a dynamic increment factor (DIF) and by a strength increment factor (SIF). According to UFC 3-340-02 [15] the DIF's are 1,19 and 1,17 for the concrete and for the steel, respectively, and SIF is taken as 1,10 in the case of the steel (Table 5-1).

Table 5-1 - Dynamic increments

Material	DIF	SIF
Concrete	1,19	-
Steel	1,17	1,10

The characteristics of the concrete shown in section 4.5 need to be incremented by the dynamic factor as presented in Table 5-2.

Table 5-2 - Concrete characteristics

Material	f_{cm} (MPa)	$f_{cm,d}$ (MPa)	f_{ctm} (MPa)	$f_{ctm,d}$ (MPa)
Concrete	50,4	59,9	3,7	4,3

For the reinforcement steel, tests were not done but the yielding stress (f_{ym}) was considered to be 540 MPa. The value of f_{ym} and its dynamic value are shown in Table 5-3.

Table 5-3 - Steel characteristics

Material	f_{ym} (MPa)	$f_{ym,d}$ (MPa)
Steel A500NR	540	695

Regarding the tubes, the characteristics need to be incremented by the dynamic factors as well (Table 5-4).

Table 5-4 - Tubes dynamic characteristics

Ø (mm)	f_y (MPa)	$f_{y,d}$ (MPa)	f_t (MPa)	$f_{t,d}$ (MPa)
48,3 e 76,1	235	302,4	360	463,3

With the incremental factors applied the same type of analytical calculation made in section 3.6 need to be done (Fig. 5-1), but now with the dynamic factors applied to consider the dynamic effect of the blast (Table 5-5).

Table 5-5 - Tubes characteristics incremented

Ø (mm)	$M_{y,d}$ [kNm]	$M_{p,d}$ [kNm]	$k_{max} = M_{p,d} / M_{y,d}$	P_d (d=0) [kN]
48,3	51,1	117,5	2,30	11,58
76,1	51,1	117,5	2,30	6,48

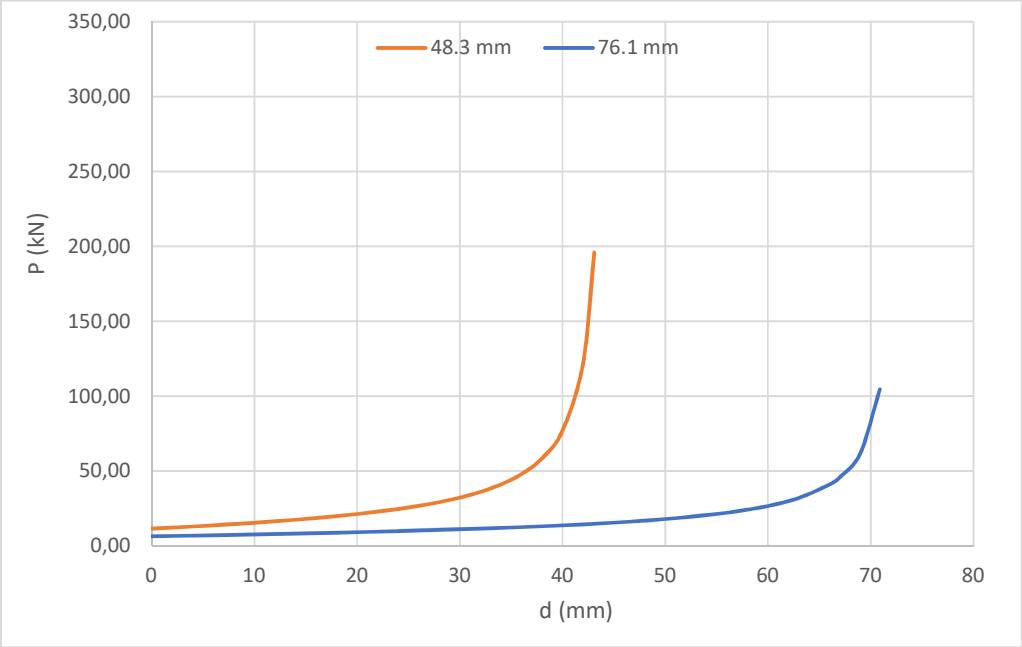

Fig. 5-1 – Dynamic force-displacement for both tubes using expression (3-18)

With this it is possible to have the integration of the graphic in Fig. 5-1 and obtain the deformation energy/displacement for each tube, as presented in Fig. 5-2.

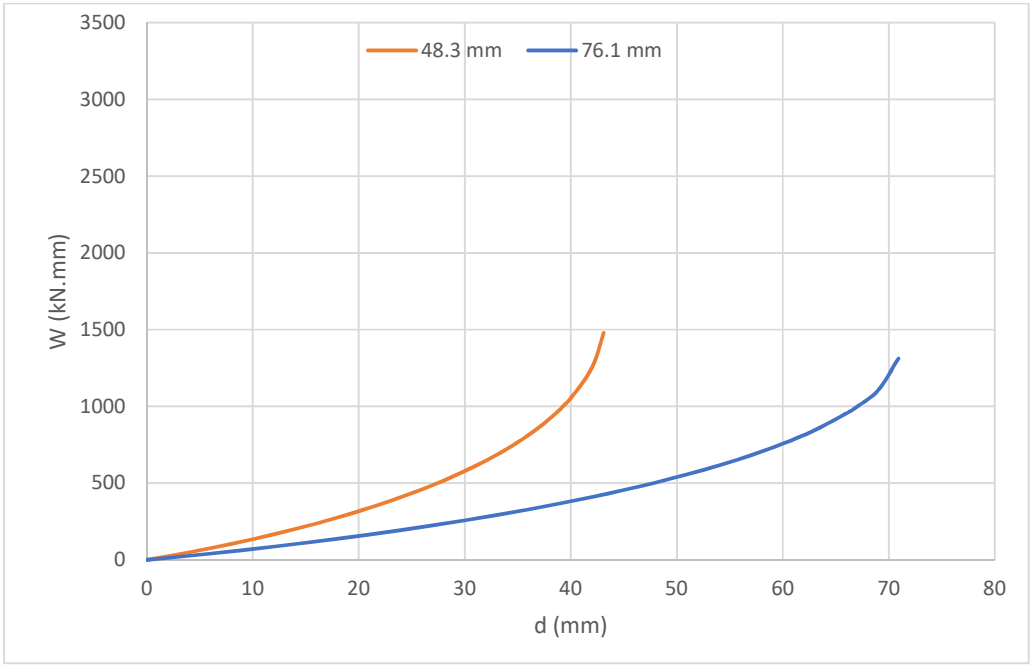

Fig. 5-2 – Energy deformation-displacement

In this graphic the tube of 48,3 mm is more efficient than the 76,1 mm diameter for lower displacements.

5.2.2. Plates and tubes on a rigid support

In this section it will be analysed how the tubes mitigate the energy of the explosion, without the deformation of the lower slab (Fig. 5-3), being the tubes the only energy dissipation system. The analysis will be done for plates on top of four tubes, with two different values of Z since the wave of the blast is not plane when it hits the model. Due to symmetry of the eight plates only two values of Z will be considered (Table 5-6).

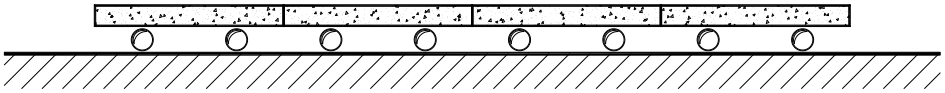

Fig. 5-3 – Plates and tubes on a rigid support

Table 5-6 - Scaled distance on the two plates analysed

Plate nº	**Z (m/Kg$^{1/3}$)**
1	1,30
2	1,18

To know the displacement that the tubes would suffer with the blast it is essential to estimate the reflected impulse in the plate (5-4) and the kinetic energy from the Eq. (3-7) with the equivalent mass for the plate estimated from (5-5). Table 5-7 shows these parameters.

$$I_r = i_r * A_{plate} \quad \textbf{(5-4)}$$

$$m_{eq} = \rho * h * A_{plate} \quad \textbf{(5-5)}$$

Table 5-7 – Calculated energy characteristics

Plate nº	I_r (kNs)	$m_{eq,}$ (kNs²/m)	T (kNmm)
1	0,321	0,114	451,7
2	0,353	0,114	548,2

Using the graphics from Fig. 5-2 it is possible to estimate the deformation the tubes need to dissipate the kinetic energy. The results are shown in Table 5-8 and it shows that the deformation of both tubes is reasonable, i.e., it is smaller than the interior diameter of each tube. For this displacement and from Fig. 5-1, it is possible to know the force needed to deform each tube, as shown in Table 5-8.

Table 5-8 – Deformation and force needed to dissipate the energy for each tube

∅ (mm)	Plate nº	W = T / 4 (kNmm)	d (mm)	P_d (kN)
48,3	1	112,9	8,55	14,91
	2	137,1	10,14	15,55
76,1	1	113,9	15,16	8,49
	2	137,1	17,94	8,88

It is also important to know the force that the four tubes apply per square meter on the lower slab, for this is necessary to multiply the force achieved in Table 5-8 by the number of tubes of each plate and divide it by the area of the plate, Eq. (5-6), the results can be seen in Table 5-9.

$$p_d = \frac{4 * P_d}{A_{plate}} \quad \textbf{(5-6)}$$

Table 5-9 – Force applied per square meter in the lower slab

Ø (mm)	Plate nº	p_d (kN/m²)	p_{dm} (kN/m²)
48,3	1	91,8	93,7
	2	95,7	
76,1	1	52,3	53,5
	2	54,7	

5.2.3. Reference slab with the designed reinforcement

The slab was designed with a reinforcement of ϕ10//0,10 (A_s = 7,85 cm²/m) and the system is designed to have a slab simply supported in two edges with 2,45 m of theoretical span.

The dynamic cracking moment may be estimated by ignoring the effect of the reinforcement in the slab by the following equation:

$$m_{cr,d} = f_{ctm,d} * W_c \quad \textbf{(5-7)}$$

In this equation the $f_{ctm,d}$ is given in Table 5.2 and W_c is the bending modulus of the section, according to the following equations.

$$W_c = \frac{b * h^2}{6} \quad \textbf{(5-8)}$$

From these expressions the dynamic cracking moment is 10,4 kNm/m. This moment corresponds to a distributed force equal to 13,9 kN/m², calculated by:

$$p_{cr,d} = \frac{8 * m_{cr,d}}{l^2} \quad \textbf{(5-9)}$$

The dynamic yielding moment of the slab may be estimated from the following expression.

$$m_{y,d} = A_s f_{y,d} b \left(d - 0{,}5 * \frac{A_s * f_{y,d}}{b * f_{cm,d}} \right) \quad \textbf{(5-10)}$$

This results on a dynamic yielding moment of 46,6 kNm/m. As the cracking moment is lower than the yield moment the slab would have a ductile behaviour and can mitigate more energy.

$$p_{y,d} = \frac{8 * m_{y,d}}{l^2} \quad \textbf{(5-11)}$$

The force needed for the reinforced steel enters in plastic behaviour is 62,1 kN/m^2.

To calculate the deformation of the reference slab it is needed to calculate the kinetic energy by the Eq. (3-7):

$$T = \frac{1}{2} * \frac{I_r^2}{m_{eq}}$$

Where the equivalent mass (m_{eq}) is:

$$m_{eq} = K_{Lm} * m_{plate} = 0{,}66 * 2500 * 10^{-3} * 0{,}12 * 2{,}45 * 2 = 0{,}97\ kN * s^2/m$$

Therefore, the kinetic energy of the slab is

$$T = \frac{1}{2} * \frac{I_r^2}{m_{eq}} = \frac{1}{2} * \frac{2{,}79^2}{0{,}970} = 3{,}99\ kNm$$

It can be considered, for simplification purposes, that the slab has a perfect-plastic behaviour and the deformation energy can be:

$$\mathrm{W} = m_{y,d} * \theta \quad \textbf{(5-12)}$$

Where θ is the rotation of that the slab suffers in the plastic hinge at mid-span, obtained by:

$$\theta = \frac{4 * a_{max}}{l} \quad \textbf{(5-13)}$$

Considering the principle of energy conservation, the maximum deformation can be calculated by:

$$a_{max} = \frac{\mathrm{W} * l}{4 * m_{y,d}} = 52\ mm \quad \textbf{(5-14)}$$

5.2.4. Slab behaviour with the mass of the plates

If we assume that the tubes are rigid, i.e., they do not dissipate any energy, the mass of the system is higher and the kinetic energy is smaller. In this case, the energy dissipated by the slab reinforcement is smaller, as well as the maximum displacement at mid span. The equivalent mass in this case is multiplied by a factor (K_{Lm}) to convert the properties of the real to the equivalent system, this factor is the quotient between the mass factor and the charge factor, the used value for the plastic regime is 0,66. The values will then be the following:

$$m_{eq} = K_{Lm} * m_{plate} = 0{,}66 * 2500 * 10^{-3} * (0{,}12 + 0{,}07) * 2{,}45 * 2 = 1{,}54\ [kN * s^2]$$

$$T = \frac{1}{2} * \frac{I_r^2}{m_{eq}} = \frac{1}{2} * \frac{2{,}79^2}{1{,}54} = 2{,}51\ kNm$$

$$a_{max} = \frac{W * l}{4 * m_{y,d}} = 33\ mm$$

5.2.5. Slab with the designed reinforcement protected by dissipation system

This dissipation system is designed to protect the lower slab, i.e., to dissipate all the energy coming from a blast. This is only possible if the lower slab is stronger than the tubes on top of it. The tubes dissipate energy by deformation and, to do so, the force applied by the tubes to the slab needs to be lower than the slab yielding.

The force in the tubes necessary to dissipate the blast energy was calculated in section 5.2.2, this value may be compared with the force needed to crack the slab and the force that will lead the reinforcement to yielding (Table 5-10) .

Table 5-10 – Comparison of the tube forces with the cracking and yielding slab forces

Ø (mm)	p_d (kN/m²)	$p_{cr,d}$ (kN/m²)	$p_{y,d}$ (kN/m²)
48,3	93,7	13,88	81,76
76,1	53,5		

The force that any of the tubes need to dissipate the energy of the blast is higher than the one needed to crack the slab. So, in any case, the slab will crack due to blast.

The yielding force of the slab is lower in the case of tubes with 48,3 mm diameter and is higher in the 76,1 mm. This means that in the case of the slab with the 76,1 mm diameter tubes the slab will crack but, after the blast these cracks close without plastification of the slab.

In the case of the tubes with 48,3 mm diameter the reinforcing steel will plastify, and the cracks will remain opened after blast. In this case, the problem is more complex because there are two systems dissipating energy (the tubes and the slab reinforcement) instead of only one. The quantification of the percentage of energy dissipated by each one of the systems is a more complex problem and is not in the scope of this work since the purpose is to reduce the damage in the slab, without plastification of the slab reinforcement, by energy dissipation of the tubes. This technique is named capacity design.

5.3. **Real behaviour of the models**

The tested slabs had a reinforcement of ϕ5//0,10 (A_s = 1,96 cm/m², instead of 7,85 cm/m²). So, the resistance of the slab is much lower than expected. The considerations regarding the system installed are the same as in section 5.2.3.

The cracking moment is the same as in section 5.2.3, because for this moment the reinforcement steel does not enter in the calculation, that is equal to 10,4 kNm.

To calculate the yielding moment with this area of steel it will be used Eq. (5-10) from which it is obtained that $m_{y,d}$ is 12,1 kNm/m, which is inferior than the expected but still higher than the cracking moment. This means that the slab will still have a ductile behaviour. This yield moment corresponds to a $p_{y,d}$ of 16,1 kN/m^2, which is the yielding force of the slab.

The same consideration taken in section 5.2.3 can also be taken in this case, that the slab, for simplification, as a perfect-plastic behaviour, and the Eq. (5-12) can be used to calculate the deformation of the slab.

5.3.1. Model FS1 – Reference model

The model FS1 was tested to determine the damage caused by the blast in a single slab and compare the results with the damage of the models with the dissipation devices. The damages are quantified in terms of deformation and cracking.

Using the same equivalent mass and kinetic energy used in section 5.2.3 it is possible to calculate the slab's deformation.

Using the Eq. (5-14) a deformation of 202 mm was obtained. Comparing this value with the obtained result in section 4.4, which is about 25 mm, this value is about 8 times lower than the expected one, the explanation for this result can be that the slab deformed until it reach the measuring system, which made the slab have another support and stop deforming.

5.3.2. Dynamic behaviour of the used steel tubes

The tubes used in tests had mechanical characteristics much different from the ordered ones and the tube with 76,1 mm diameter had 3,2 mm wall thickness

instead of 2,6 mm, comparing Fig. 5-4 with Fig. 5-1 the difference can be seen. For these tubes the calculations done in section 5.2.1 were done. Table 5-11 shows the characteristics of the tubes used.

Table 5-11 - Characteristics of the tubes used

Ø (mm)	Wall thickness (mm)	$M_{y,d}$ (kNm)	$M_{p,d}$ (kNm)	$k_{max} = M_{p,d} / M_{y,d}$	P_d (d=0) (kN)
48,3	2,6	98,5	192,5	1,95	22,33
76,1	3,2	148,9	266,9	1,79	19,82

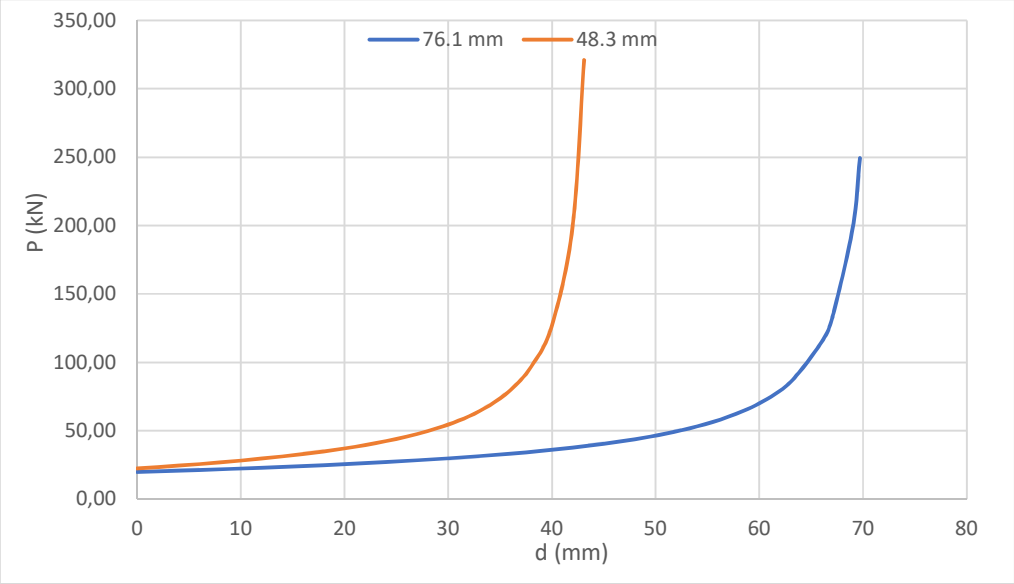

Fig. 5-4 – Dynamic force-displacement for the tubes used in the tests

As in section 5.2.1 from the integration of the graphic in Fig. 5-7 it is possible to have a deformation energy/displacement for each tube, presented in Fig. 5-8

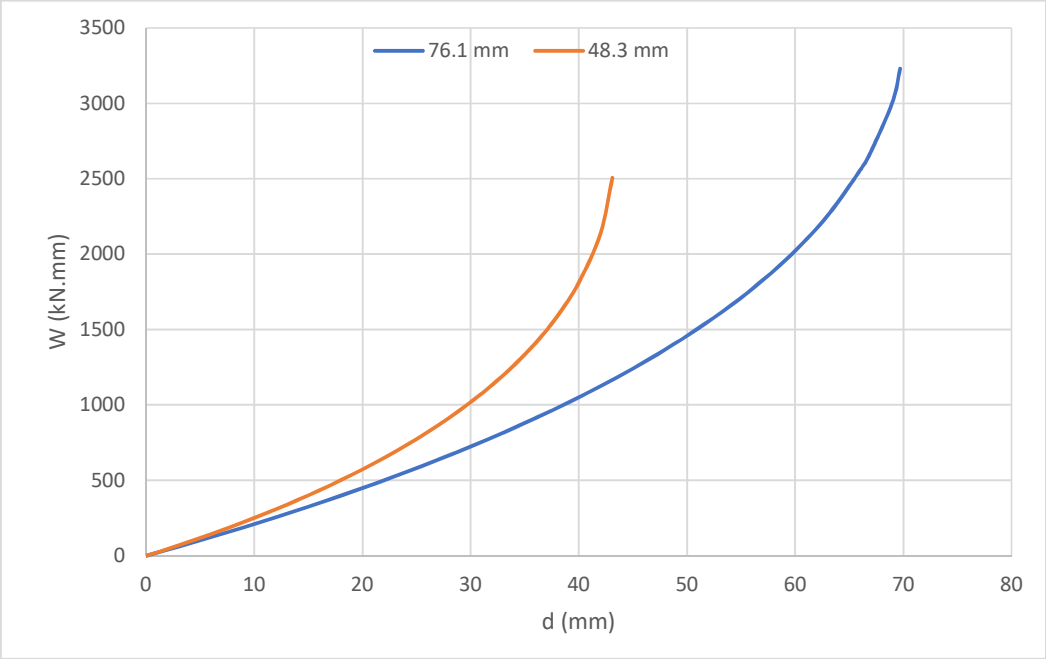

Fig. 5-5 – Energy deformation-displacement of the tubes used in the tests

In this graphic the tube of 48,3 mm outer diameter is more efficient than the 76,1 mm diameter for the smaller displacements. The tube of 76,1 mm is more efficient only for displacements greater than 65 mm.

With the same blast parameters used in section 5.2.2 and the same rigid support, calculations were done to evaluate the used tubes (Table 5-12).

Table 5-12 – Deformation and force of the tubes

Ø (mm)	Plate nº	W = T / 4 (kNmm)	a (mm)	P_d (kN)
48,3	1	112,9	4,8	24,88
	2	137,1	5,8	25,31
76,1	1	113,9	5,5	21,14
	2	137,1	6,6	21,39

As done before in section 5.2.2, the force that the four tubes apply per square meter on the lower slab is necessary, the results can be seen in Table 5-13.

Table 5-13 – Force applied per square meter in the lower slab

Ø (mm)	Plate nº	p_d (kN/m²)	p_{dm} (kN/m²)
48,3	1	153,1	154,4
	2	155,8	
76,1	1	130,1	130,9
	2	131,6	

5.3.3. Models FS2 and FS3

For these models the equivalent mass needs to be calculated again, adding the mass in the section 5.2.3 and the one in the section 5.2.2, multiplying by the number of plates, resulting in the total mass of the system.

$$m_{eq} = 8 * m_{eq,plates} + m_{eq,slab} = 1{,}54[kN * s^2]$$

Knowing that the yielding force of the slab is $p_{y,d}$, this is the maximum force in the tubes and corresponds to a certain value of energy dissipation. The remnant of the blast energy needs to be dissipated by plastification of the slab. This force of the slab is 16,1 kN/m², as seen in section 5.3, which means that the maximum force that the tubes will dissipate is 2,6 kN (Eq. (5-6)). This force is not enough to deform the tubes (Fig. 5-4), so all the energy will be dissipated by the slab. Although this, the difference in the equivalent mass in relation to the reference slab reduces the expected deformation of these models to be around 122 mm, which is lower than the FS1 model.

5.4. **Results interpretation**

Table 5-14 presents all the results of the experimental campaign performed in Campo Militar de Santa Margarida and described in section 4.4.

Table 5-14 – Resume of the slabs damages

Test	W_{TNT} (Kg)	R (m)	System	Cracking (mm)	Deformation (mm)	
					Maximum	Residual
FS1	4,50	1,85	Ref.	0,25	25	10
FS2	4,50	1,85	76,1 mm tubes	0,15	40	7
FS3	4,50	1,85	48,3 mm tubes	0,20	29	5
FS4	4,50	1,85	Ref.	0,10	25	8

The tests show that the maximum theoretical deformation isn´t reached in any test, being the highest in the second test with the tubes of 76,1 mm reaching 40 mm, this difference can be explained by the imprecision of the methods used in the calculation of the impulse of the explosion and in the measurement of the deflections.

The tubes in the middle of the slab, the ones that are closer to the charge, had larger deformations, meaning that the shock wave is not plane, as said in section 5.1. The graphics in Fig. 5-7 and Fig. 5-8 show the deformations of the tubes, according to their position on the slab, as shown in Fig. 5-6.

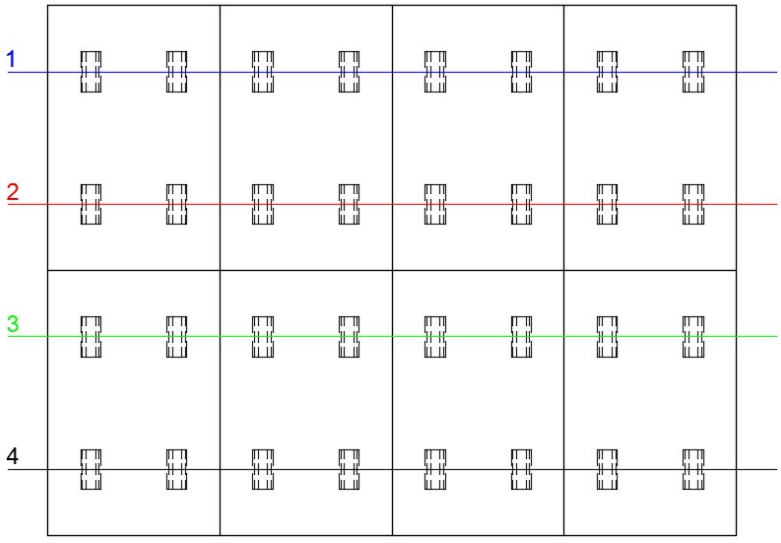

Fig. 5-6 - Position of the tubes on the slab for Fig. 5-7 and Fig. 5-8

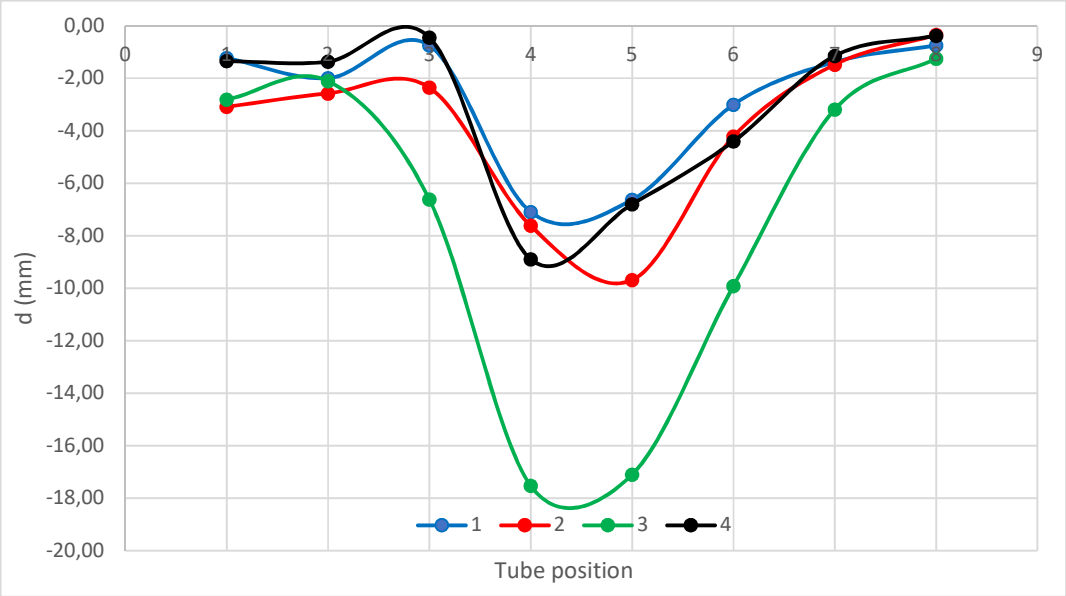

Fig. 5-7 - Graphic with the residual deformation of the 76,1 mm tubes after blast.

Comparing the reference slab and the slab with the 76,1 mm tubes the following numbers can be seen:

- Both slabs have shown innumerable cracks in the lower and the sides of the slabs;
- In the maximum deformation there was an increase of 15 mm in the deformation;
- The residual deformation decreased;
- The visible cracks reduced from 0,25 mm to 0,15 mm;
- The deformation of the tubes was as high 17,53 mm.

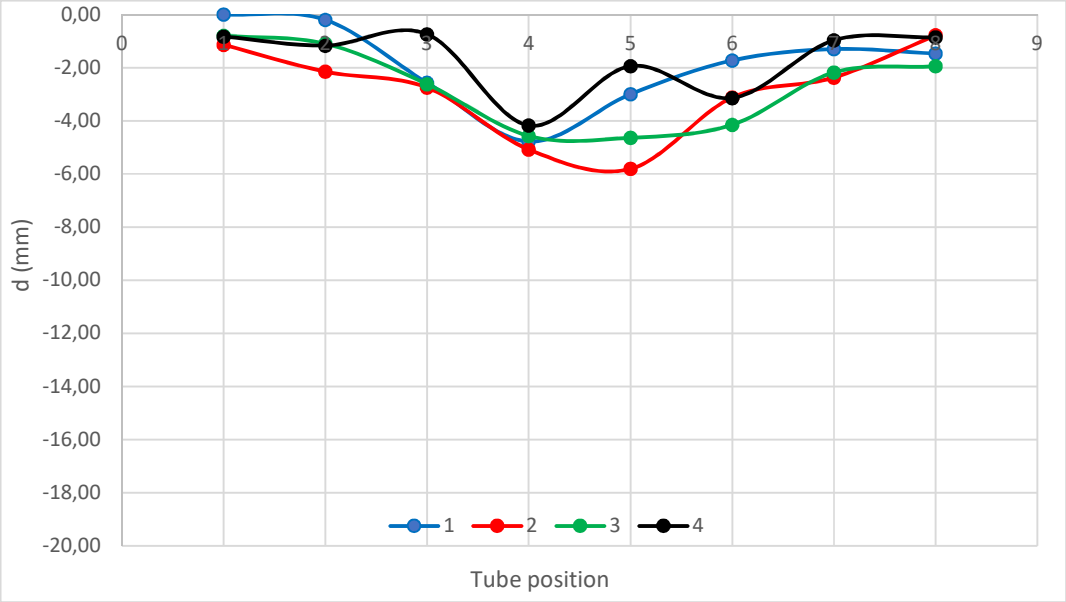

Fig. 5-8 - Graphic with the residual deformation of the 48,3 mm tubes after blast.

Comparing now the reference slab with the slab with the 48,3 mm tubes these are the facts:

- Both slabs had numerous cracks in the lower and the sides of the slabs;
- In the maximum deformation there was an increase of 4 mm in the deformation;
- The residual deformation decreased;
- The visible cracks reduced from 0,25 mm to 0,20 mm;
- The deformation of the tubes was as high 5,81 mm.

It may be concluded that the use of both systems is an improvement to a normal slab in case of explosion blast. Although this experimental campaign did not get good results, it may be concluded that these systems can be an improvement to this type of structures. The tubes in the designed specimens would dissipate most of the energy of the blast, protecting the slab from large deformations.

6. CONCLUSIONS AND FUTURE DEVELOPMENTS

The dissertation follows the work developed by João [16], Gonçalves [11], Rebelo [17] and Nabais [14], in the development of a system to protect concrete structures against terrorist attacks. In the present dissertation a system that allows the concrete structure to stay almost undamaged was developed, sacrificing the tubes for the security of the building.

6.1. Conclusions

The first conclusion that can be taken from this research is that in the steel tubes the force needed to deform totally the tube is always increasing, this is due to the drift of the force towards the plastic hinge that forms in the tube.

The numerical model, made using the ADINA software, presents a good approximation on the elastic phase. In the plastic phase the model does not consider the change of the point of application of the force, so in this phase distances from the test results.

The analytical model presented in this research gives a good approximation to the plastic phase. This similarity with the real test makes it a good model to design slabs stronger than the tubes.

The designed slabs and tubes show that this solution can be very effective for the protection of buildings from a blast. The difference of the deformations considering only the tubes and the plates was much lower than the ones considering the slab and the plates without the tubes, even though the equivalent mass of the second system is higher. These results show that the proposed system may be a good improvement in the protection of structures, allowing the structure to remain undamaged.

The experimental campaign was based on four tests, where in two of them two systems, one with 48,3 mm tubes and another with 76,1 mm tubes, were installed to compare the damage done in each slab, two other slabs were tested as reference. In all the tests the blast consisted on 6 Kg of Eurodyn 2000, which is equivalent to 4,5 Kg of TNT, at 1,85 m from the top of the slab. The experimental results in the large scale specimens show that, although the slabs were less resistant than they should be, the tubes still dissipated some energy of the blast making.

The results show that the tubes and the concrete slabs need to be a very precisely designed to comply with the capacity design, i.e., the force developed in the tubes to dissipate the energy shall not exceed the yielding force of the slab reinforcement.

6.2. **Future developments**

A lot of research has been carried out on the protection of buildings against blast actions. The following research developments are proposed for the future:

- To develop a practical system to fix the tubes to building concrete walls;
- To implement a numerical model to design the system and to study the variations of all the components;
- To perform an experimental campaign to confirm experimentally the design of the dissipating system.

BIBLIOGRAPHY

[1] Study of Terrorism and Responses to Terrorism; *Annex of Statistical Information*; Country Reports on Terrorism; Maryland, 2017.

[2] Reid S.; Reddy T.; *Experimental investigation of inertia effects in one dimensional metal ring systems subject to end impact*, International Journal of Impact Engineering, 1983.

[3] Reid S.; Reddy T.; *Phenomena associated with crushing of metal tubes between rigid plates*, International Journal of Impact Engineering, 1980.

[4] Guruprasad S.; Mukherjee A.; *Layered sacrificial claddings under blast loading Part I - Analytical studies*; International Journal of Impact Engineering, 2000.

[5] Guruprasad S.; Mukherjee A.; *Layered sacrificial claddings under blast loading Part II - Analytical studies*; International Journal of Impact Engineering, 2000.

[6] Palanivelu S. et al*; Performance of Sacrificial Cladding Structure Made of Empty Recyclable Metal Beverage Cans under Large-Scale Air Blast Load; Applied Mechanics and Materials*, Jul. 2011.

[7] Lavarnway D.; Pollino M.; *Mitigation of Air-Blast Pressure Impulses on Building Envelopes through Blast Resistant Ductile Connectors*; Journal of Engineering and Architecture, 2015.

[8] ACI; *318-08: Building Code Requirements for Structural Concrete and Commentary.* American Concrete Institution, 2008.

[9] Kinney G.; Graham K.; *Explosive Shocks in Air*. Berlin, Heidelberg: Springer Berlin Heidelberg, 1985.

[10] Mlakar P.; Barker D.; *Blast Phenomena*, Handbook for Blast Resistant

Design of Buildings, 2010.

[11] Gonçalves M.; *Reforço de placas de betão armado com argamassas armadas para acções de explosão*; Dissertação para obtenção do grau de Mestre em Engenharia Civil, FCT-UNL, 2015.

[12] IPQ; *NP EN ISO 6892-1: 2012 - Materiais metálicos Ensaio de tração Parte 1: Método de ensaio à temperatura ambiente*; IPQ - Instituito Português da Qualidade, 2012.

[13] IPQ; *NP EN 1992-1-1: 2010 - Eurocódigo 2 – Projecto de estruturas de betão Parte 1-1: Regras gerais e regras para edifícios*; IPQ - Instituito Português da Qualidade, 2010.

[14] Nabais D.; *Desenvolvimento de um Sistema Inovador de Proteção de Estruturas de Betão contra Explosões*; Dissertação para obtenção do grau de Mestre em Engenharia Militar, IST, 2016.

[15] UFC 3-340-02; *Structures to Resist the Effects of Accidental Explosions*; Structures Congress 2011; 2008.

[16] João T.; *Comportamento de painéis sandwich de betão armado sujeitos a ações de explosão*; Dissertação para obtenção do grau de Mestre em Engenharia Civil, FCT-UNL, 2016.

[17] Rebelo, H; *Numerical Simulation of Blast on Fibre Grout Strengthened RC Panels*; Dissertação para obtenção do grau de Mestre em Engenharia Civil, FCT-UNL, 2015.

[18] Needham, C.; *Blast Waves, Shock Wave and High Pressure Phenomena*; Springer Heidelberg, 2010

ANNEX A – DESIGNED LARGE SCALE MODELS

ÀTT

ACADEMIA MILITAR

DATA: 09 de Junho de 2017

ASSUNTO: N/ ORÇAMENTO Nº**248/2017 –Revisão 01**

FORNECIMEO DE PEÇAS PREFABRICADAS

1º- Este orçamento compreende o fornecimento (nas nossas instalações) de:

- **PAINÉIS e PLACAS** prefabricadas em betão armado (C25/30 - A500NR, A500ER), com acabamento liso em betão de cimento cinzento (à cor natural) na face superior e acabamento areado na face interior, conforme desenhos anexos recebidos com a consulta de Vexas e mapa de quantidades no pto 5.º deste orçamento.
- **CUBOS** prefabricados em betão armado (C25/30), com acabamento liso betão nas faces visíveis, conforme desenhos anexos recebidos com a consulta de Vexas e mapa de quantidades no pto 5.º deste orçamento.
- **TUBOS** sem costura em aço conforme desenhos recebidos com a consulta de Vexas e mapa de quantidades no pto 5.º deste orçamento.

2º- Não está incluído neste orçamento:

- **O Transporte do material acima referido.**
- **Quaisquer tratamentos de proteção, barramentos, pinturas, pinturas impermeabilizantes e/ou envernizamentos.**

- **Quaisquer alterações (dimensões e características) em relação aos desenhos recebidos.**

- **Quaisquer trabalhos não explicitamente referidos nos pontos 1º e 2º. descarga e montagem dos referidos elementos.**

- **Alterações às quantidades.**

3º- Considerações Gerais:

- Os prefabricados em betão cinzento poderão apresentar ligeiras diferenças de tonalidade entre peças, como é próprio e característico deste material.

4º- Prazos de execução:

- A combinar em caso de adjudicação de acordo com a disponibilidade fabril.

5º- Nestas condições o valor deste orçamento é de:

Conforme Quadro:

	PEÇA/ REF.ª	QUANTIDADE [un]	L1 [m]	L2 [m]	Esp. [m]	Preço [€/un]	Totais/Tipo [€]
Conforme desenhos recebidos no email de 30-04-2017	Painel 1	4	2,60	2,00	0,12	230,00 €	920,00 €
Conforme desenhos recebidos no email de 06-06-2017	Placa 1	8	0,65	1,00	0,10	37,00 €	296,00 €
Conforme desenhos recebidos no email de 06-06-2017	Placa 2	16	0,65	1,00	0,06	34,00 €	544,00 €
	cubos	30	0,15	0,15	0,15	0,00 €	0,00 €
Conforme desenhos recebidos no email de 02-05-2018	Painel 2	8	2,60	2,00	0,12	185,00 €	1 480,00 €
				VALOR TOTAL PLACAS E PAINÉIS			3 240,00 €

	PEÇA/ REF.ª	QUANTIDADE [un]	Preço [€/un]	Totais/Tipo [€]
Conforme desenhos recebidos no email de 06-06-2017	Tubos DIN 2448 ST37 76.1*2.6 com 150mm	69	2,94 €	202,65 €
	Tubos DIN 2448 ST37 48.3*2.6 com 150mm	37	3,83 €	141,76 €
	1/4 Tubos DIN 2448 ST37 76.1*2.6 com 400mm	4	2,14 €	8,54 €
	1/2 Tubos DIN 2448 ST37 48.3*2.6 com 400mm	4	3,89 €	15,55 €
			VALOR TOTAL TUBOS ST37	368,51 €
			TOTAL DA PROPOSTA	3 608,51 €

- Sobre os valores acima indicados incidirá o I.V.A. à taxa legal em vigor
- Não haverá lugar a qualquer retenção percentual sobre o valor das facturas

6º- Garantias Bancárias:

- Caso o cliente assim o pretenda, a Concremat prestará uma Garantia Bancária até 5% do valor dos nossos trabalhos e por um prazo máximo de 5 anos após a conclusão dos nossos trabalhos. Os custos desta Garantia Bancária serão suportados diretamente pelo nosso cliente.

7º- Condições de pagamento:

- As facturas serão pagas até 60 (sessenta) dias da sua data de emissão, através de uma operação de "confirming" bancário do pagamento das facturas.
- Se por razões que nos forem alheias existir impossibilidade de entregar o material em obra, a factura dirá respeito ao material fabricado existente nas nossas instalações.
- Se por razões que nos forem alheias, nos for solicitada a suspensão dos trabalhos, será facturada imediatamente a fase seguinte àquela em que se encontram

8º- Fazem parte integrante desta proposta os desenhos anexos recebidos com a consulta de V.Exas.

9º- A desistência de toda ou parte da encomenda, após a adjudicação, obrigará da parte de V.Exas. à liquidação de todos os encargos decorrentes dos custos já efectuados (estudos, preparação da encomenda e moldes). Em caso de atrasos na obra não imputáveis à CONCREMAT, será facturado o material em stock nas nossas instalações

10º- Prazos de validade:

- A presente proposta é válida por 30 (trinta) dias a contar desta data.

11º- Esta proposta considerar-se-á aceite por V. Exas. após confirmação por escrito e com a informação do banco favorável à operação de confirming do valor total acordado

Na expectativa de merecer a v/ atenção, apresentamos os nossos melhores cumprimentos.

De V. Exas.

Atentamente

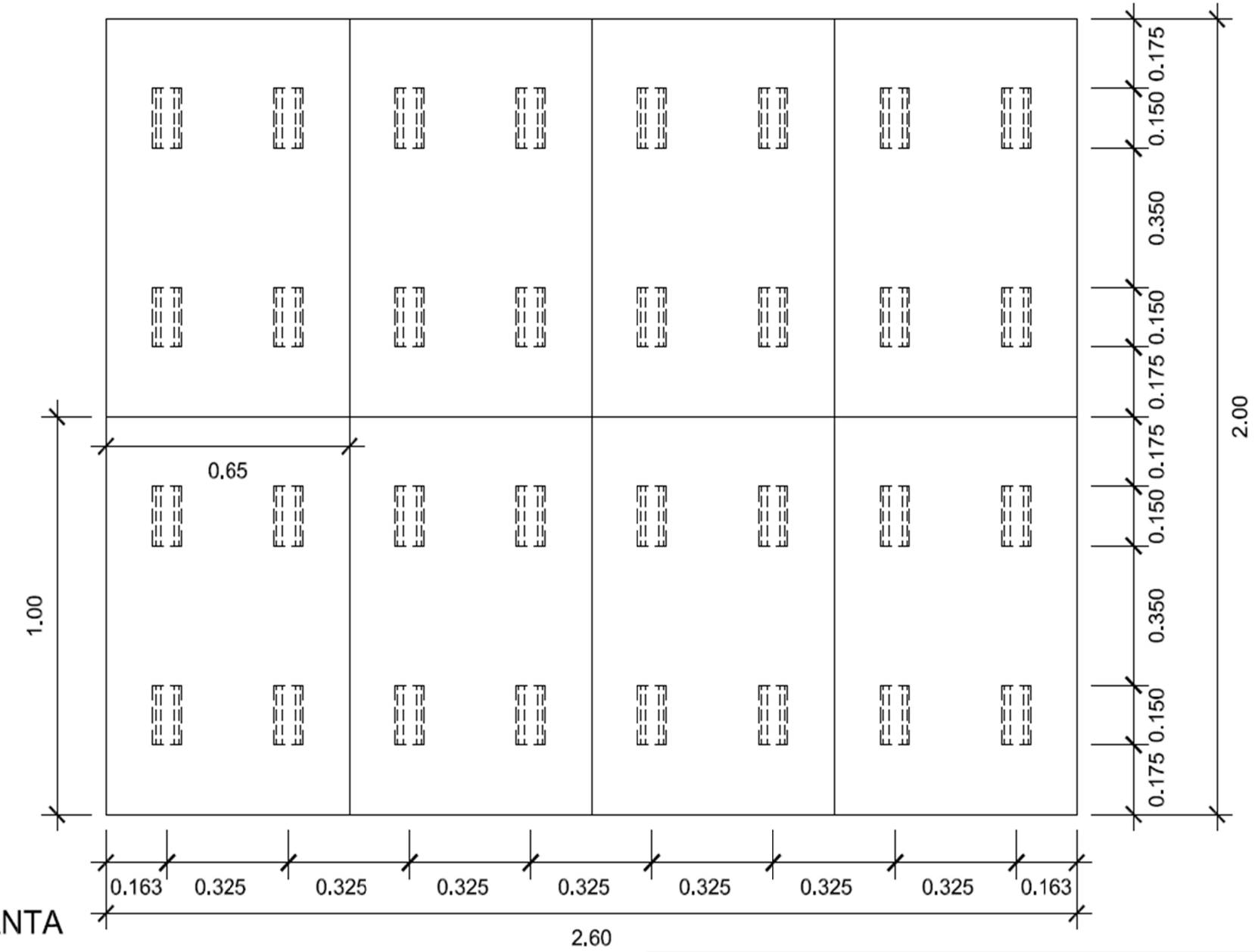

PLANTA

Betão C25/30 rec: 25mm
Aço A500NR e A500ER
Tubos sem costura em aço ST37

PROJETO Frederico Soares
Des. 01A Esc.: 1/10 06/06/2017

08

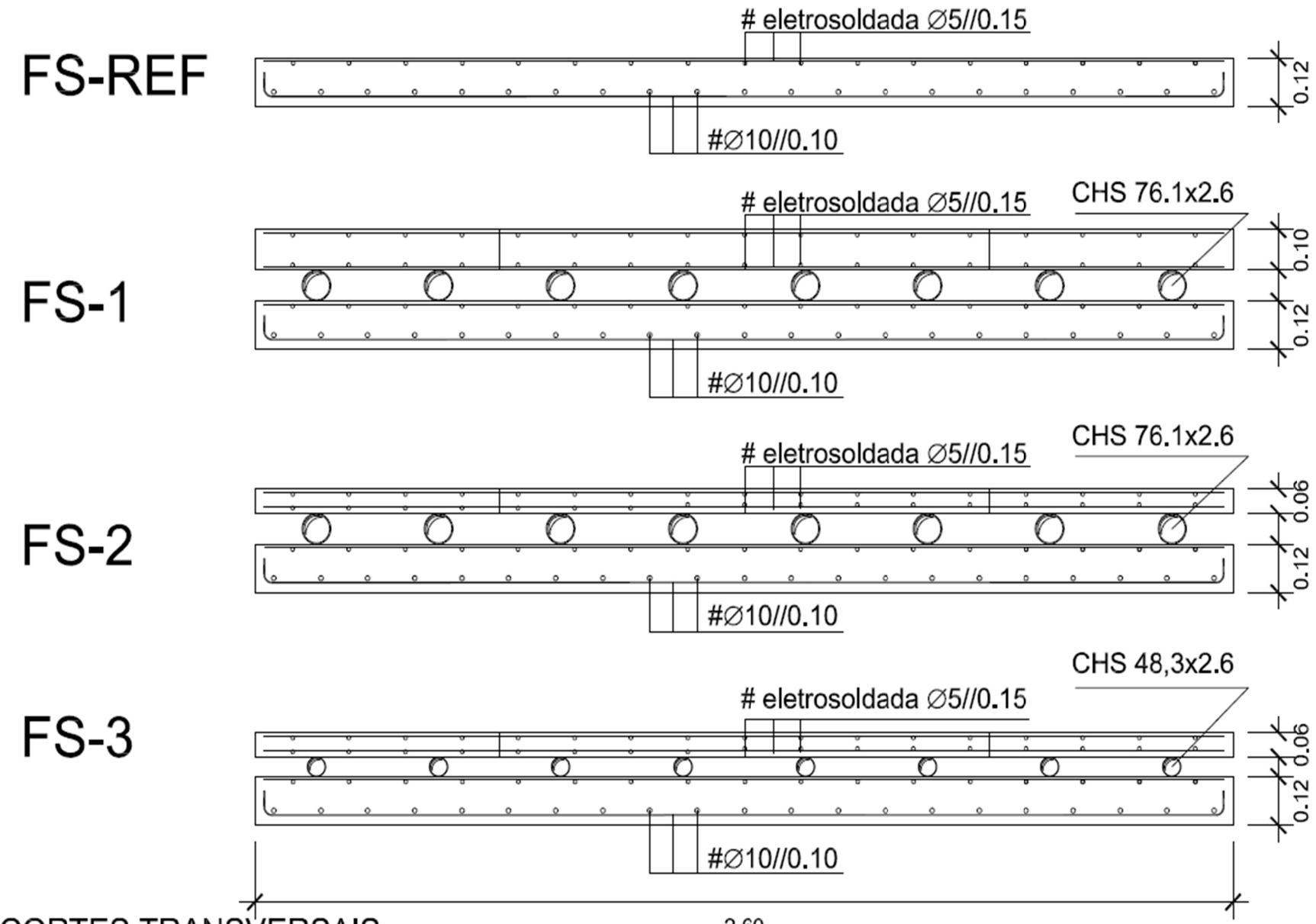

CORTES TRANSVERSAIS

Betão C25/30 rec: 25mm
Aço A500NR e A500ER
Tubos sem costura em aço ST37

PROJETO Frederico Soares
Des. 02A Esc.: 1/10 06/06/2017

QUANTIDADES

FS-REF

1 x Placa 2.60x2.0x0.12m + *6 cubos c/ 150 mm de aresta*
Armadura inferior #∅10//0.10
Armadura superior #eletrosoldada ∅5//0.15

FS-1

1 x Placa 2.60x2.0x0.12m + *6 cubos c/ 150 mm de aresta*
Armadura inferior #∅10//0.10
Armadura superior #eletrosoldada ∅5//0.15
8 x Placas 1.0x0.65x0.10m
Armadura 2x #eletrosoldada ∅5//0.15
32 x tubos CHS 76.1x2.6 c/ 150mm de comprimento

FS-2

1 x Placa 2.60x2.0x0.12m + *6 cubos c/ 150 mm de aresta*
Armadura inferior #∅10//0.10
Armadura superior #eletrosoldada ∅5//0.15
8 x Placas 1.0x0.65x0.06m
Armadura 2x #eletrosoldada ∅5//0.15
32 x tubos CHS 76.1x2.6 c/ 150mm de comprimento

FS-3

1 x Placa 2.60x2.0x0.12m + *6 cubos c/ 150 mm de aresta*
Armadura inferior #∅10//0.10
Armadura superior #eletrosoldada ∅5//0.15
8 x Placas 1.0x0.65x0.06m
Armadura 2 x #eletrosoldada ∅5//0.15
32 x tubos CHS 48,3x2.6 c/ 150mm de comprimento

Betão C25/30 rec: 25mm
Aço A500NR e A500ER
Tubos sem costura em aço ST37

5 x tubos CHS 48,3x2.6 c/ 150mm de comprimento
5 x tubos CHS 76.1x2.6 c/ 150mm de comprimento

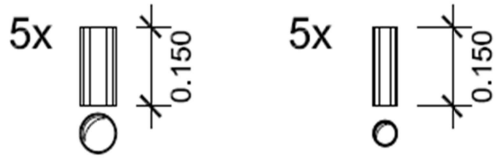

4 x quartos de tubo CHS 76.1x2.6
c/ 400mm de comprimento

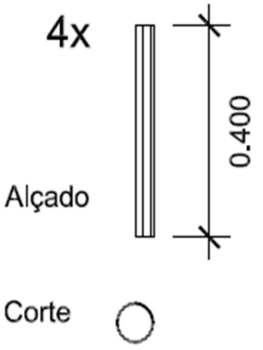

4 x metades de tubo CHS 48.3x2.6
c/ 400mm de comprimento

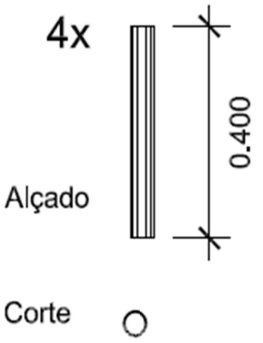

PROJETO Frederico Soares

Quantidades (A) 06/06/2017

ANNEX B – LARGE SCALE TESTS

Annex B.1 – FS1 reference model

FICHA DE ENSAIO Nº1

I. DADOS GERAIS

1. Data/Hora do ensaio: 2 de out. 2017 às 11:00h	**2. Local do ensaio:** Campo Militar Sta. Margarida
3. Investigadores presentes: **FCT-NOVA:** Prof. Doutor Válter Lúcio, Frederico Soares **Exército Português:** Capitão José Basto, Capitão João Marques **4. Outras presenças:** José Gaspar **Apoios:** Companhia de Engenharia/BrigMec – 2 Retroescavadoras, 1 SecEng, Ambulância, Bombeiros **5. Redação da Ficha:** Frederico Soares	

6. Descrição geral e Objectivo do ensaio
FS.1 – ensaio de laje de referência, simplesmente apoiada em dois bordos paralelos, com um vão livre de 2.30m e carga explosiva de 6 kg a 1,85 m de distância. O objectivo deste ensaio é analisar os efeitos que as cargas resultantes desta explosão geram na laje de referência, para comparação com os efeitos em lajes reforçadas com a camada de sacrifício.

II. DESCRIÇÃO DOS ELEMENTOS ENSAIADOS

7. Tipologia do(s) elemento(s) ensaiados									
☐ **Fundação**	☐ **Pilar**	☐ **Viga**	☒ **Laje**	☐ **Parede resistente**	☐ **Parede não resistente**	☐ **Muro**	☐ **Pórtico 2D**	☐ **Pórtico 3D**	☐ **Outro** _____

8. Esboço do(s) elemento(s) ensaiado(s)

(Configuração do ensaio, incluindo medidas geométricas [m] e sentido de impacto)

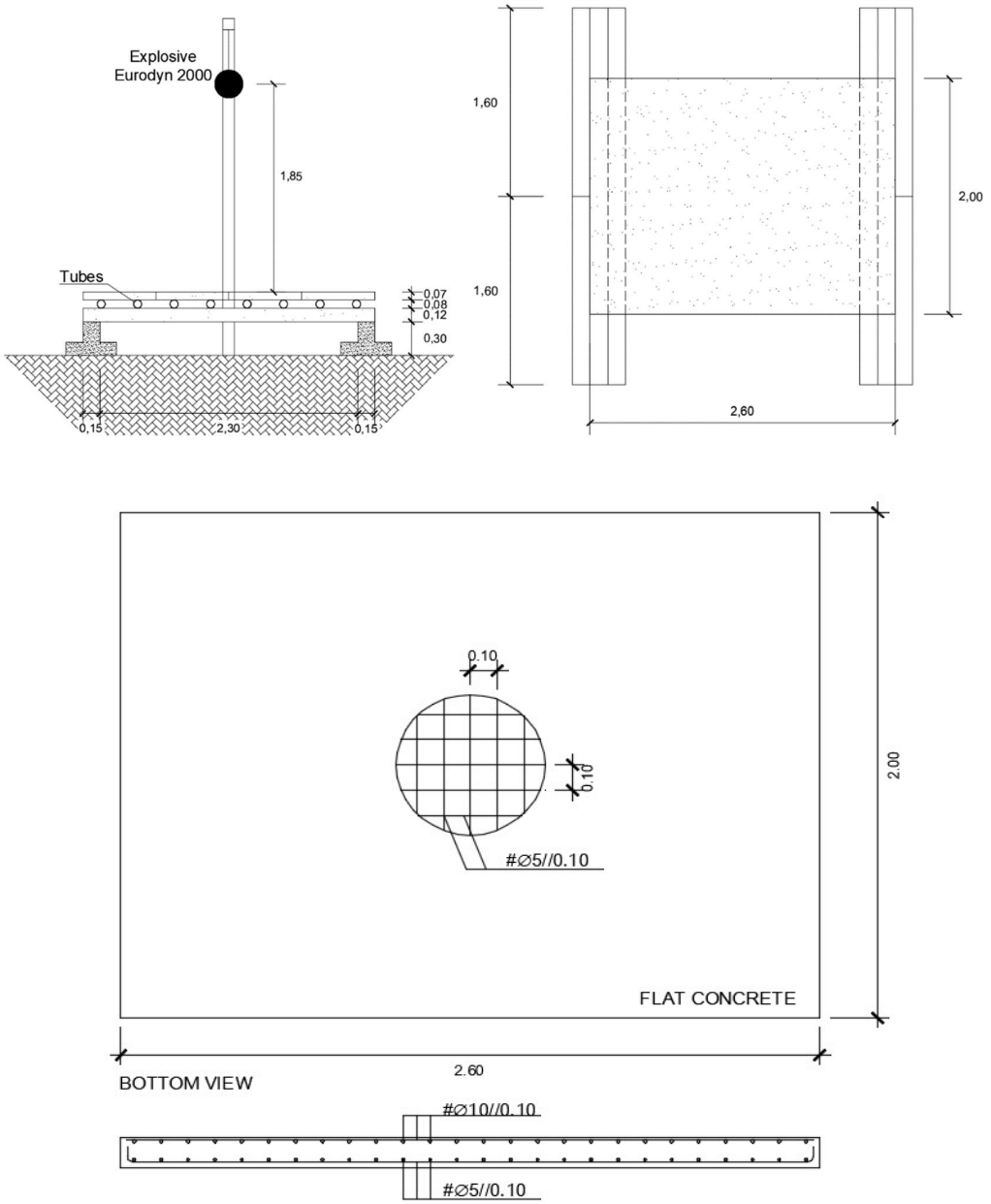

Armaduras na Laje

9. Caraterísticas dos materiais do(s) elemento(s) ensaiados		
Betão C 25/ 30 Resultado dos cubos aos 102 dias: Rcp= 56 MPa ☒Não deteriorado ☐Deterioração Física:_____ ☐Deterioração Química:_____ ☐Deterioração por Corrosão	**Armaduras** Malha Electro soldada: A 500 ER Aço em Armadura Ordinária: A500 NR **Recobrimento** (e)0.03[m]	**Materiais e tipologia de Reforço** Esta laje não foi reforçada para servir de referência para as outras lajes com reforço.

III. DESCRIÇÃO DA(S) CARGA(S) EXPLOSIVA(S) UTILIZADA(S)

10. Caraterísticas do(s) explosivo(s)		
Eurodyn 2000 ☒120g X ___50_____*(nº petardos)* ☐200g X _____*(nº petardos)* ☐1kg X _____*(nº petardos)* ☐1kg a granel X _____*(nº sacos)* ☐Outro: _____ (nº petardos)	**PE-4A** ☐230g X _____*(nº velas)* ☐Outro:_____	☐**Outro:** *(emulsão, hidrogel, etc.)*

11. Esboço do(s) explosivos(s) utilizados(s)

(Configuração geométrica. Incluindo medidas e orientação face ao elemento ensaiado)

12. Caraterísticas do meio			
Distância ao alvo: 1,85 [m]	Altura ao solo: 2,27 [m]	Temperatura: 30 [°C]	Humidade: desc [%]

IV. MONITORIZAÇÃO

13. Descrição do sistema *(tipologia, funcionamento, etc.)*

O sistema de monitorização consiste em até 10 hastes de arame cravados numa espuma expandida, permitindo medir a deformação instantânea da laje aquando da explosão pela diferença de comprimento livre das hastes entre o antes e o após o ensaio.

14. Esboço do sistema *(localização e orientação de sensores, etc.)*

(ver secção 8)

V. REGISTO FOTOGRÁFICO

15. Pré-ensaio *(3 Fotos - Vista geral, elementos ensaiados e cargas utilizadas)*


Sítio para descarga de álbum completo: _____

16. Pós-ensaio *(3 Fotos - Vista geral, elementos ensaiados e projeções)*

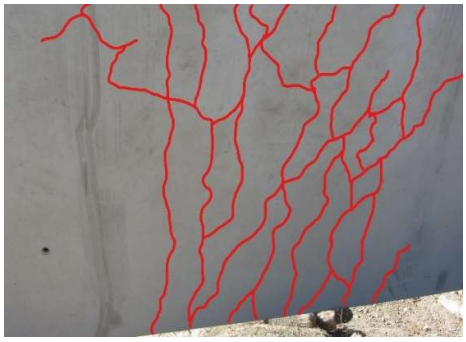


Sítio para descarga de álbum completo: _____

VI. RESULTADOS DOS ENSAIOS

17. Efeitos observados
O ensaio provocou fendilhação e deformação do modelo por flexão a meio vão. Fendilhação (abertura e orientação): foram observadas diversas fendas nos bordos e na face inferior. Deformação (máxima instantânea e permanente): A deformação instantânea medida nas hastes foi de 10 a 30 mm e a deformação residual medida com régua de 2m e fita métrica na face foi entre 6 mm e 10 mm. Outros Reutilização do(s) elemento(s) após ensaio: ☒**Sim** ☐**Não** ☐ **Limitado:**_____

VII. PARÂMETROS ESTIMADOS DA ONDA DE CHOQUE (Refª: TM 5-1300)

Distância reduzida Z= **1,12** [m/Kg$^{1/3}$]	Pressão de pico reflectida Pr= **4,05 x10^3** [KPa]	Pressão de pico incidente Ps$_0$= **786,223** [KPa]
Impulso reflectido Ir= **567,954** [KPa-ms]	Impulso incidente Is= **110,189** [KPa-ms]	Tempo de chegada da onda ta= **1,92** [ms]
Duração da fase positiva t$_0$= **0,38** [ms]	Velocidade da onda U= **0,97** [m/ms]	Comprimento da onda Lw= **0,37** [m]

VIII. OBSERVAÇÕES *(Referir melhorias futuras, entre outras)*

Annex B.2 – FS2 model with 76,1 mm tubes

FICHA DE ENSAIO Nº2

I. DADOS GERAIS

1. Data/Hora do ensaio: 2 de out. 2017 às 15:00h	**2. Local do ensaio:** Campo Militar Sta. Margarida
3. Investigadores presentes: **FCT-NOVA:** Prof. Doutor Válter Lúcio, Frederico Soares **Exército Português:** Capitão José Basto, Capitão João Marques **4. Outras presenças:** José Gaspar **Apoios:** Companhia de Engenharia/BrigMec – 2 Retroescavadoras, 1 SecEng, Ambulância, Bombeiros **5. Redação da Ficha:** Frederico Soares	

6. Descrição geral e Objectivo do ensaio
FS.2 – ensaio de laje de com a primeira camada de sacrifício, com tubos de 76,1 mm, simplesmente apoiada em dois bordos paralelos, com um vão livre de 2.30m e carga explosiva de 6 kg a 1,85 m de distância. O objectivo deste ensaio é analisar a deformação que os tubos de 76,1 mm têm de modo a que a laje não sofra tantos danos

II. DESCRIÇÃO DOS ELEMENTOS ENSAIADOS

7. Tipologia do(s) elemento(s) ensaiados									
☐ **Fundação**	☐ **Pilar**	☐ **Viga**	☒ **Laje**	☐ **Parede resistente**	☐ **Parede não resistente**	☐ **Muro**	☐ **Pórtico 2D**	☐ **Pórtico 3D**	☐ **Outro** _____

8. Esboço do(s) elemento(s) ensaiado(s)

(Configuração do ensaio, incluindo medidas geométricas [m] e sentido de impacto)

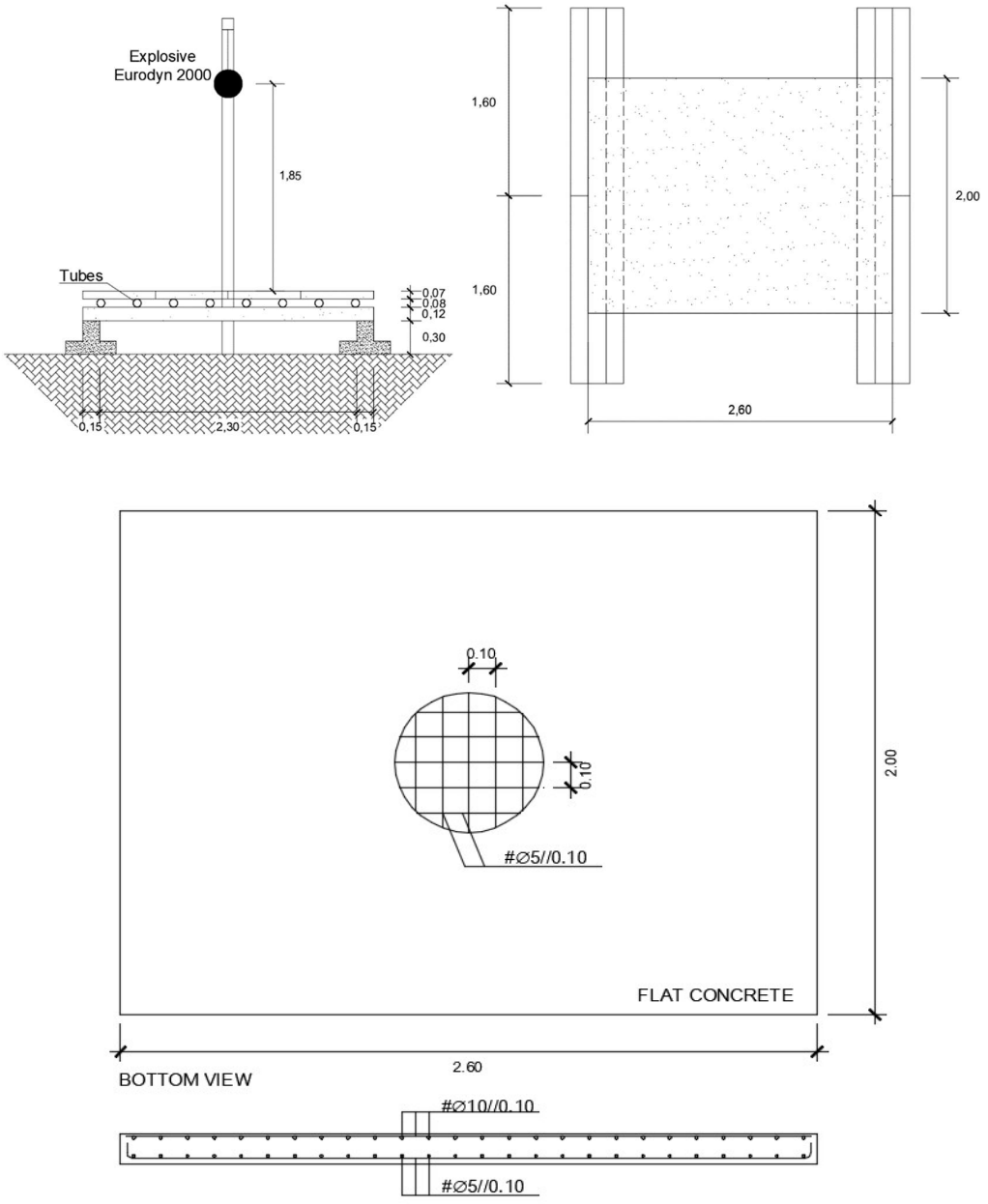

Armaduras na Laje

9. Caraterísticas dos materiais do(s) elemento(s) ensaiados		
Betão C 25/ 30 Resultado dos cubos aos 102 dias: Rcp= 56 Mpa ☒Não deteriorado ☐Deterioração Física:_____ ☐Deterioração Química:_____ ☐Deterioração por Corrosão	**Armaduras** Malha Electro soldada: A 500 ER Aço em Armadura Ordinária: A500 NR **Recobrimento** (e)0.03[m]	**Materiais e tipologia de Reforço** Esta laje foi reforçada com uma camada de sacrifício composta por 32 tubos de 76,1 mm.

III. DESCRIÇÃO DA(S) CARGA(S) EXPLOSIVA(S) UTILIZADA(S)

10. Caraterísticas do(s) explosivo(s)		
Eurodyn 2000 ☒120g X ___50_____*(nº petardos)* ☐200g X _____*(nº petardos)* ☐1kg X _____*(nº petardos)* ☐1kg a granel X _____*(nº sacos)* ☐Outro: _____ (nº petardos)	**PE-4A** ☐230g X _____*(nº velas)* ☐Outro:_____	☐**Outro:** *(emulsão, hidrogel, etc.)*

11.Esboço do(s) explosivos(s) utilizados(s)

(Configuração geométrica. Incluindo medidas e orientação face ao elemento ensaiado)

12. Caraterísticas do meio			
Distância ao alvo: 1,85 [m]	Altura ao solo: 2,27 [m]	Temperatura: 30 [°C]	Humidade: desc [%]

IV. MONITORIZAÇÃO

13. Descrição do sistema *(tipologia, funcionamento, etc.)*

O sistema de monitorização consistiu em até 10 hastes de arame cravados numa espuma expandida, permitindo medir a deformação instantânea da laje aquando da explosão pela diferença de comprimento livre das hastes entre o antes e o após o ensaio.

14. Esboço do sistema *(localização e orientação de sensores, etc.)*

(ver secção 8)

V. REGISTO FOTOGRÁFICO

15. Pré-ensaio *(3 Fotos - Vista geral, elementos ensaiados e cargas utilizadas)*


Sítio para descarga de álbum completo: _____

16. Pós-ensaio *(3 Fotos - Vista geral, elementos ensaiados e projeções)*


Sítio para descarga de álbum completo: _____

VI. RESULTADOS DOS ENSAIOS

17. Efeitos observados
O ensaio provocou fendilhação e deformação do modelo por flexão a meio vão. Fendilhação (abertura e orientação): foram observadas diversas fendas nos bordos e na face inferior. Deformação (máxima instantânea e permanente): A deformação instantânea medida nas hastes foi de 30 a 40 mm e a deformação residual medida com régua de 2m e fita métrica na face foi entre 7 mm e 4 mm. Outros Reutilização do(s) elemento(s) após ensaio: ☒**Sim** ☐**Não** ☐ **Limitado:**_____

VII. PARÂMETROS ESTIMADOS DA ONDA DE CHOQUE (Refª: TM 5-1300)

Distância reduzida Z= **1,12** [m/Kg$^{1/3}$]	Pressão de pico reflectida Pr= **4,05 x10^3** [KPa]	Pressão de pico incidente Ps$_0$= **786,223** [KPa]
Impulso reflectido Ir= **567,954** [KPa-ms]	Impulso incidente Is= **110,189** [KPa-ms]	Tempo de chegada da onda ta= **1,92** [ms]
Duração da fase positiva t$_0$= **0,38** [ms]	Velocidade da onda U= **0,97** [m/ms]	Comprimento da onda Lw= **0,37** [m]

VIII. OBSERVAÇÕES *(Referir melhorias futuras, entre outras)*

Annex B.3 – FS3 model with 48,3 mm tubes

FICHA DE ENSAIO Nº3

I. DADOS GERAIS

1. Data/Hora do ensaio: 2 de out. 2017 às 16:00h	**2. Local do ensaio:** Campo Militar Sta. Margarida
3. Investigadores presentes: **FCT-NOVA:** Prof. Doutor Válter Lúcio, Frederico Soares **Exército Português:** Capitão José Basto, Capitão João Marques **4. Outras presenças:** José Gaspar **Apoios:** Companhia de Engenharia/BrigMec – 2 Retroescavadoras, 1 SecEng, Ambulância, Bombeiros **5. Redação da Ficha:** Frederico Soares	

6. Descrição geral e Objectivo do ensaio
FS.3 – ensaio de laje de com a primeira camada de sacrifício, com tubos de 48,3 mm, simplesmente apoiada em dois bordos paralelos, com um vão livre de 2.30m e carga explosiva de 6 kg a 1,85 m de distância. O objectivo deste ensaio é analisar a deformação que os tubos de 48,3 mm têm de modo a que a laje não sofra tantos danos

II. DESCRIÇÃO DOS ELEMENTOS ENSAIADOS

7. Tipologia do(s) elemento(s) ensaiados

☐ Fundação	☐ Pilar	☐ Viga	☒ Laje	☐ Parede resistente	☐ Parede não resistente	☐ Muro	☐ Pórtico 2D	☐ Pórtico 3D	☐ Outro _____

8. Esboço do(s) elemento(s) ensaiado(s)

(Configuração do ensaio, incluindo medidas geométricas [m] e sentido de impacto)

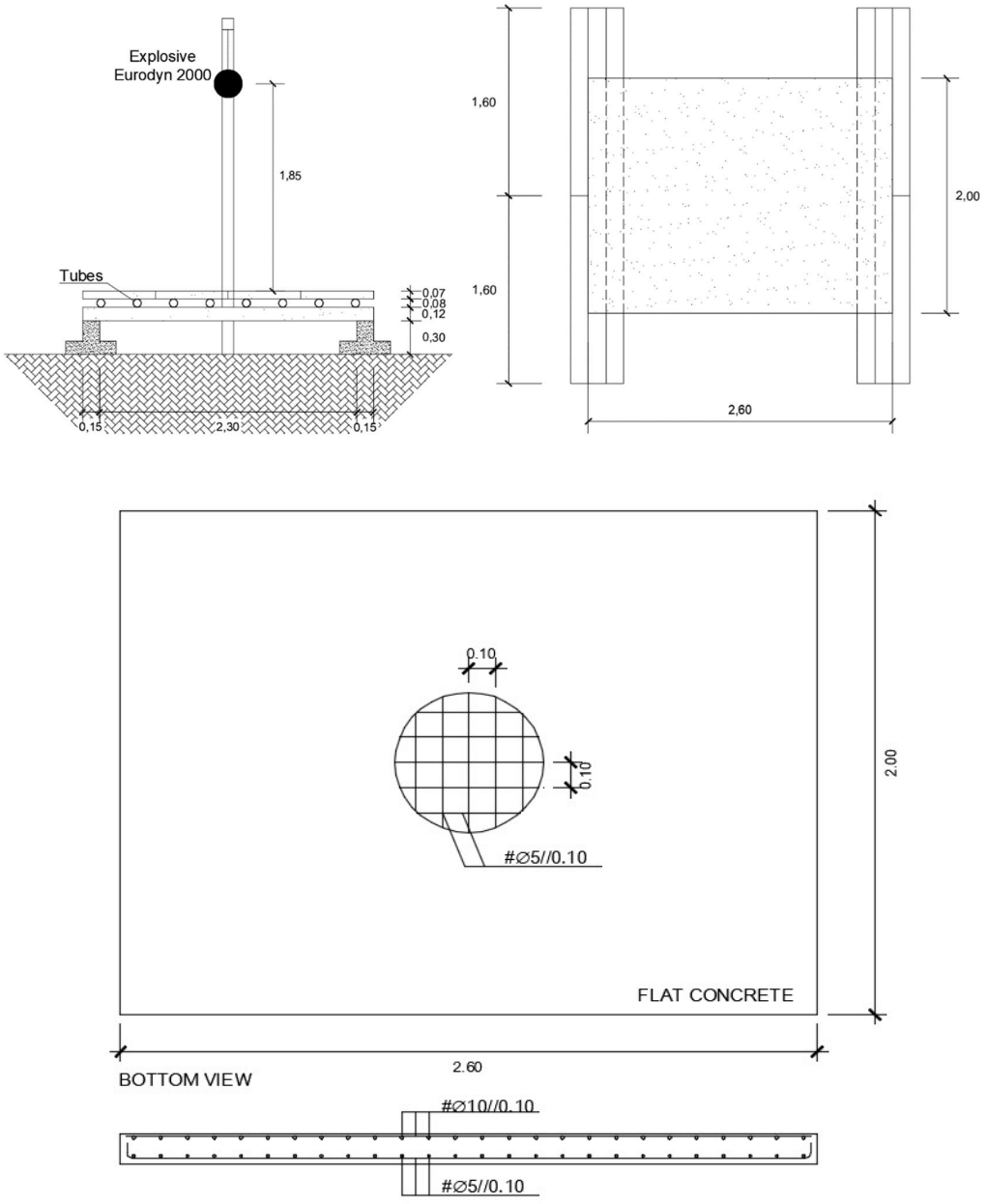

Armaduras na Laje

9. Caraterísticas dos materiais do(s) elemento(s) ensaiados		
Betão C 25/ 30 Resultado dos cubos aos 102 dias: Rcp= 56 Mpa ☒Não deteriorado ☐Deterioração Física:_____ ☐Deterioração Química:_____ ☐Deterioração por Corrosão	**Armaduras** Malha Electro soldada: A 500 ER Aço em Armadura Ordinária: A500 NR **Recobrimento** (e)0.03[m]	**Materiais e tipologia de Reforço** Esta laje foi reforçada com uma camada de sacrifício composta por 32 tubos de 48,3 mm.

III. DESCRIÇÃO DA(S) CARGA(S) EXPLOSIVA(S) UTILIZADA(S)

10. Caraterísticas do(s) explosivo(s)		
Eurodyn 2000 ☒120g X ___50_____*(nº petardos)* ☐200g X _____*(nº petardos)* ☐1kg X _____*(nº petardos)* ☐1kg a granel X _____*(nº sacos)* ☐Outro: _____ (nº petardos)	**PE-4A** ☐230g X _____*(nº velas)* ☐Outro:_____	☐**Outro:** *(emulsão, hidrogel, etc.)*

11. Esboço do(s) explosivos(s) utilizados(s)

(Configuração geométrica. Incluindo medidas e orientação face ao elemento ensaiado)

12. Caraterísticas do meio			
Distância ao alvo: 1,85 [m]	Altura ao solo: 2,27 [m]	Temperatura: 30 [°C]	Humidade: desc [%]

IV. MONITORIZAÇÃO

13. Descrição do sistema *(tipologia, funcionamento, etc.)*

O sistema de monitorização consistiu em até 10 hastes de arame cravados numa espuma expandida, permitindo medir a deformação instantânea da laje aquando da explosão pela diferença de comprimento livre das hastes entre o antes e o após o ensaio.

14.Esboço do sistema *(localização e orientação de sensores, etc.)*

(ver secção 8)

V. REGISTO FOTOGRÁFICO

15. Pré-ensaio *(3 Fotos - Vista geral, elementos ensaiados e cargas utilizadas)*

Sítio para descarga de álbum completo: _____

16. Pós-ensaio *(3 Fotos - Vista geral, elementos ensaiados e projeções)*

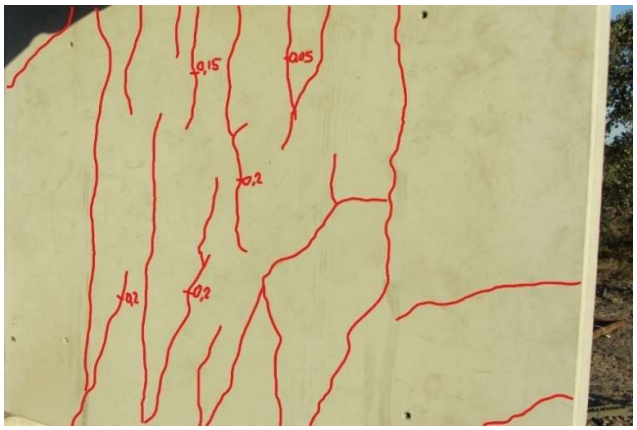

Sítio para descarga de álbum completo: _____

VI. RESULTADOS DOS ENSAIOS

17. Efeitos observados
O ensaio provocou fendilhação e deformação do modelo por flexão a meio vão. Fendilhação (abertura e orientação): foram observadas diversas fendas nos bordos e na face inferior. Deformação (máxima instantânea e permanente): A deformação instantânea medida nas hastes foi de 16 a 29 mm e a deformação residual medida com régua de 2m e fita métrica na face foi de 5 mm. Outros Reutilização do(s) elemento(s) após ensaio: ☒**Sim** ☐**Não** ☐ **Limitado:**_____

VII. PARÂMETROS ESTIMADOS DA ONDA DE CHOQUE (Refª: TM 5-1300)

Distância reduzida Z= **1,12** [m/Kg$^{1/3}$]	Pressão de pico reflectida Pr= **4,05 x10^3** [KPa]	Pressão de pico incidente Ps$_0$= **786,223** [KPa]
Impulso reflectido Ir= **567,954** [KPa-ms]	Impulso incidente Is= **110,189** [KPa-ms]	Tempo de chegada da onda ta= **1,92** [ms]
Duração da fase positiva t$_0$= **0,38** [ms]	Velocidade da onda U= **0,97** [m/ms]	Comprimento da onda Lw= **0,37** [m]

VIII. OBSERVAÇÕES *(Referir melhorias futuras, entre outras)*

Annex B.4 – FS4 reference model

FICHA DE ENSAIO Nº4

I. DADOS GERAIS

1. Data/Hora do ensaio: 2 de out. 2017 às 17:00h	**2. Local do ensaio:** Campo Militar Sta. Margarida
3. Investigadores presentes: **FCT-NOVA:** Prof. Doutor Válter Lúcio, Frederico Soares **Exército Português:** Capitão José Basto, Capitão João Marques **4. Outras presenças:** José Gaspar **Apoios:** Companhia de Engenharia/BrigMec – 2 Retroescavadoras, 1 SecEng, Ambulância, Bombeiros **5. Redação da Ficha:** Frederico Soares	

6. Descrição geral e Objectivo do ensaio
FS.1 –ensaio de laje de referência, simplesmente apoiada em dois bordos paralelos, com um vão livre de 2.30m e carga explosiva de 6 kg a 1,85 m de distância. O objectivo deste ensaio é analisar os efeitos que as cargas resultantes desta explosão geram na laje de referência, para comparação e confirmação do ensaio nº1 (FS1) com os efeitos em lajes reforçadas com a camada de sacrifício.

II. DESCRIÇÃO DOS ELEMENTOS ENSAIADOS

7. Tipologia do(s) elemento(s) ensaiados									
☐ **Fundação**	☐ **Pilar**	☐ **Viga**	☒ **Laje**	☐ **Parede resistente**	☐ **Parede não resistente**	☐ **Muro**	☐ **Pórtico 2D**	☐ **Pórtico 3D**	☐ **Outro** _____

8. Esboço do(s) elemento(s) ensaiado(s)

(Configuração do ensaio, incluindo medidas geométricas [m] e sentido de impacto)

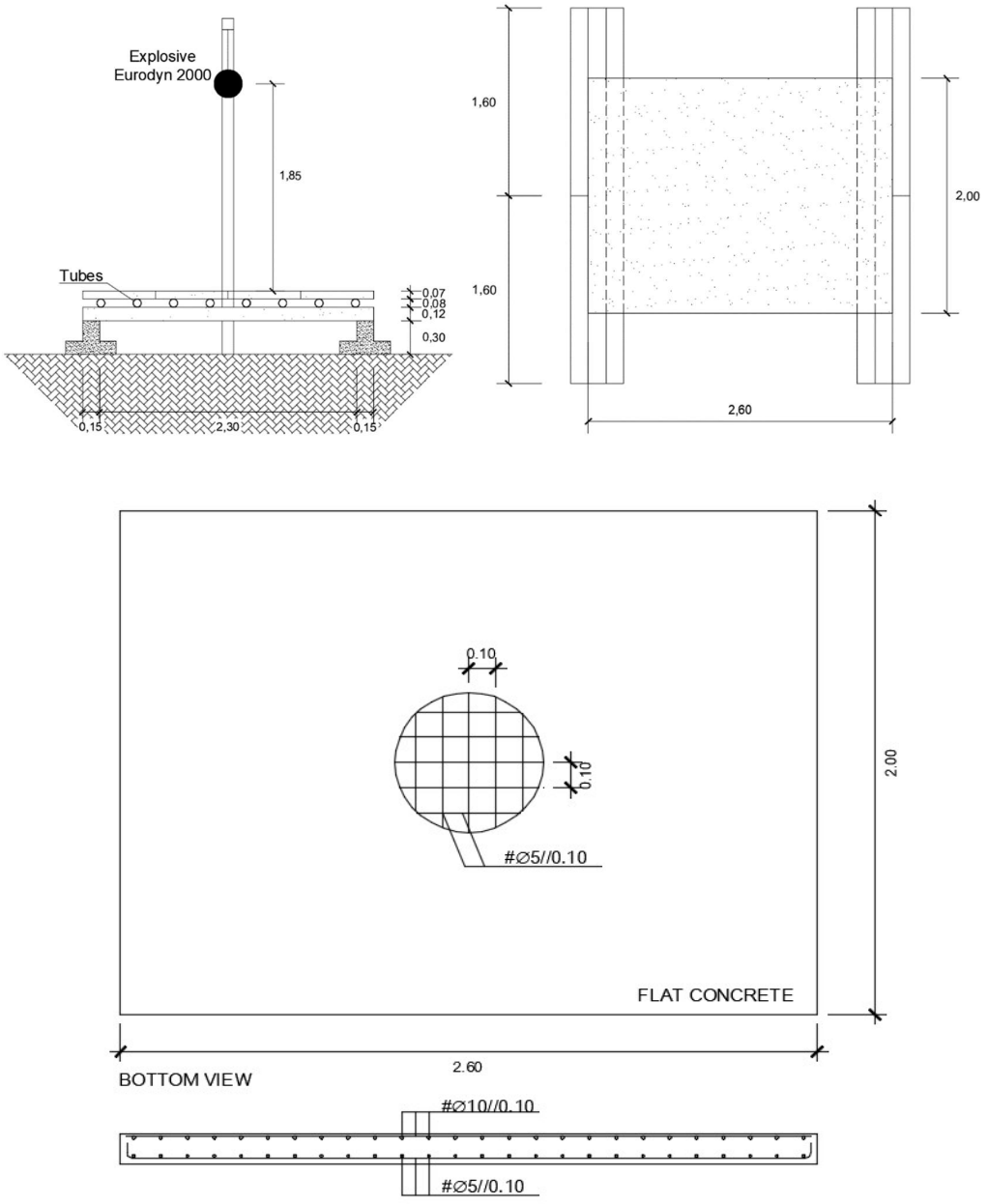

Armaduras na Laje

9. Caraterísticas dos materiais do(s) elemento(s) ensaiados		
Betão C 25/ 30 Resultado dos cubos aos 102 dias: Rcp= 56 Mpa ☒Não deteriorado ☐Deterioração Física:_____ ☐Deterioração Química:_____ ☐Deterioração por Corrosão	**Armaduras** Malha Electro soldada: A 500 ER Aço em Armadura Ordinária: A500 NR **Recobrimento** (e)0.03[m]	**Materiais e tipologia de Reforço** Esta laje não foi reforçada para servir de referência para as outras lajes com reforço.

III. DESCRIÇÃO DA(S) CARGA(S) EXPLOSIVA(S) UTILIZADA(S)

10. Caraterísticas do(s) explosivo(s)		
Eurodyn 2000 ☒120g X ___50_____*(nº petardos)* ☐200g X _____*(nº petardos)* ☐1kg X _____*(nº petardos)* ☐1kg a granel X _____*(nº sacos)* ☐Outro: _____ (nº petardos)	**PE-4A** ☐230g X _____*(nº velas)* ☐Outro:_____	☐**Outro:** *(emulsão, hidrogel, etc.)*

11.Esboço do(s) explosivos(s) utilizados(s)

(Configuração geométrica. Incluindo medidas e orientação face ao elemento ensaiado)

12. Caraterísticas do meio			
Distância ao alvo: 1,85 [m]	Altura ao solo: 2,27 [m]	Temperatura: 30 [°C]	Humidade: desc [%]

IV. MONITORIZAÇÃO

13. Descrição do sistema *(tipologia, funcionamento, etc.)*

O sistema de monitorização consiste em até 10 hastes de arame cravados numa espuma expandida, permitindo medir a deformação instantânea da laje aquando da explosão pela diferença de comprimento livre das hastes entre o antes e o após o ensaio.

14. Esboço do sistema *(localização e orientação de sensores, etc.)*

(ver secção 8)

V. REGISTO FOTOGRÁFICO

15. Pré-ensaio *(3 Fotos - Vista geral, elementos ensaiados e cargas utilizadas)*

Sítio para descarga de álbum completo: _____

16. Pós-ensaio *(3 Fotos - Vista geral, elementos ensaiados e projeções)*

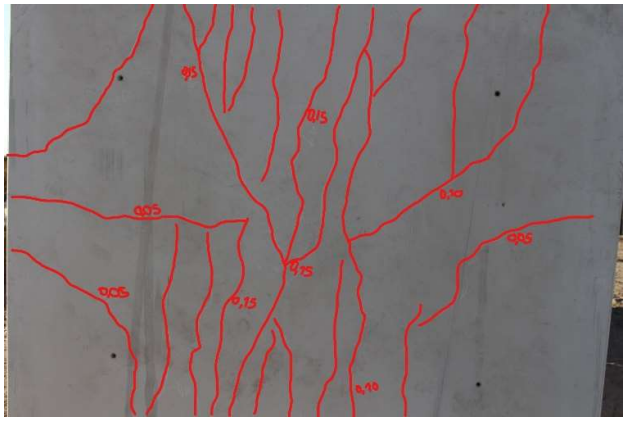

Sítio para descarga de álbum completo: _____

VI. RESULTADOS DOS ENSAIOS

17. Efeitos observados
O ensaio provocou fendilhação e deformação do modelo por flexão a meio vão. Fendilhação (abertura e orientação): foram observadas diversas fendas nos bordos e na face inferior. Deformação (máxima instantânea e permanente): A deformação instantânea medida nas hastes foi de 14 a 25 mm e a deformação residual medida com régua de 2m e fita métrica na face foi entre 7 mm e 8 mm. Outros Reutilização do(s) elemento(s) após ensaio: ☒**Sim** ☐**Não** ☐ **Limitado:**_____

VII. PARÂMETROS ESTIMADOS DA ONDA DE CHOQUE (Refª: TM 5-1300)

Distância reduzida Z= **1,12** [m/Kg$^{1/3}$]	Pressão de pico reflectida Pr= **4,05 x10^3** [KPa]	Pressão de pico incidente Ps$_0$= **786,223** [KPa]
Impulso reflectido Ir= **567,954** [KPa-ms]	Impulso incidente Is= **110,189** [KPa-ms]	Tempo de chegada da onda ta= **1,92** [ms]
Duração da fase positiva t$_0$= **0,38** [ms]	Velocidade da onda U= **0,97** [m/ms]	Comprimento da onda Lw= **0,37** [m]

VIII. OBSERVAÇÕES *(Referir melhorias futuras, entre outras)*